



Enzyme-assisted target recycling (EATR) for nucleic acid detection

Journal:	<i>Chemical Society Reviews</i>
Manuscript ID:	CS-REV-02-2014-000083.R1
Article Type:	Review Article
Date Submitted by the Author:	08-May-2014
Complete List of Authors:	Gerasimova, Yulia; University of Central Florida, Chemistry Department Kolpashchikov, Dmitry; University of Central Florida, Chemistry

Enzyme-assisted target recycling (EATR) for nucleic acid detection

Yulia V. Gerasimova* and Dmitry M. Kolpashchikov

Chemistry Department, University of Central Florida, 4000 Central Florida Blvd., Orlando, FL 32816, USA. E-mail: yugeras@gmail.com

Abstract

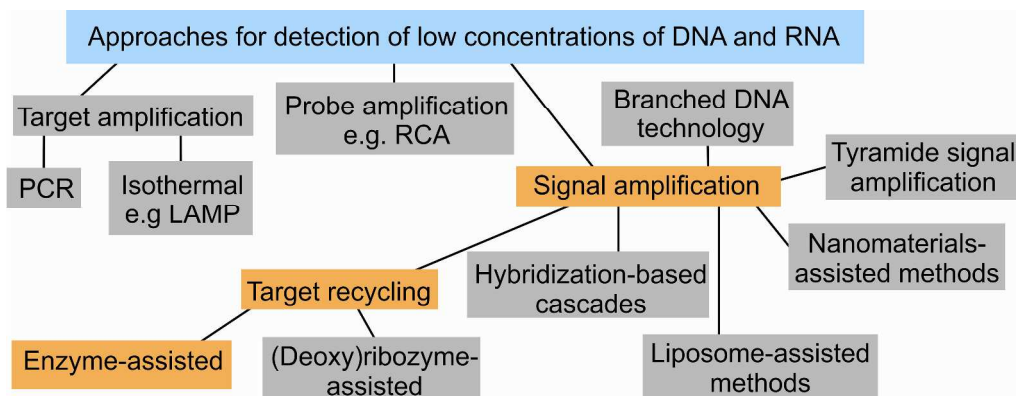
Fast, reliable and sensitive methods for nucleic acid detection are of growing practical interest with respect to molecular diagnostics of cancer, infectious and genetic diseases. Currently, PCR-based and other target amplification strategies are most extensively used in practice. At the same time, such assays have limitations that can be overcome by alternative approaches. There is a recent explosion in the design of methods that amplify the signal produced by a nucleic acid target, without changing its copy number. This review aims at systematization and critical analysis of enzyme-assisted target recycling (EATR) signal amplification technique. The approach uses nucleases to recognize and cleave the probe-target complex. Cleavage reactions produce a detectable signal. The advantages of such techniques are potentially low sensitivity to contamination, lack of the requirement of a thermal cycler. Nucleases used for ETR include sequence-dependent restriction or nicking endonucleases or sequence independent exonuclease III, lambda exonuclease, RNase H, RNase HII, AP endonuclease, duplex-specific nuclease, DNase I, or T7 exonuclease. EATR-based assays are potentially useful for point-of-care diagnostics, single nucleotide polymorphisms genotyping and microRNA analysis. Specificity, limit of detection and the potential impact of EATR strategies on molecular diagnostics are discussed.

1. EATR in the context of hybridization-based techniques for nucleic acid detection

Sensitive and specific detection of nucleic acids finds fast-growing applications in diagnostics of infectious diseases,¹⁻³ microRNA analysis,⁴⁻⁶ food control,⁷⁻⁹ epigenetics,¹⁰⁻¹² human identification in forensic investigations,¹³⁻¹⁵ as well as in biomedical research.¹⁶⁻¹⁸ For these purposes, methods that use hybridization of oligonucleotide probes to the analyzed DNA or RNA target have been widely used. The probes are pre-designed to bind complementary fragments of target nucleic acids followed by detection of the probe-target complexes. Among the variety of hybridization probe of particular importance are those that report the presence of targets in mix-and-read formats by generating a fluorescent, chemiluminescent, electrochemical or visual signals without the need for time-consuming and effort-intensive processing of the samples. The examples of mix-and-read hybridization probes include the broad variety of binary (split) probes,¹⁹⁻²¹ molecular beacon (MB) probes²²⁻²⁴ and their variations.²⁵⁻²⁷

Since hybridization probes form 1:1 complex with their targets to produce a signal, the limits of detection (LOD) for the probes with non-radioactive signal readout are not good enough for detection of low-abundant nucleic acids. To improve the LOD of the hybridization assays, they are used in combination with target amplification, probe amplification or signal amplification strategies (Scheme 1). Target amplification allows replication of a DNA fragment of interest 10^8 - 10^9 -fold to achieve target concentration high enough to be detected with conventional approaches (e.g. gel electrophoresis/staining or fluorescent probes). A classic example of target amplification is polymerase chain reaction (PCR),²⁸⁻³¹ which is a gold standard in DNA detection in terms of LOD. However, it requires an expensive thermal cycler, which

limits its application in point-of-care settings. Isothermal target amplification methods have emerged recently as thermal cycler-free alternatives of PCR.³²⁻³⁵ The examples of such methods include helicase-dependent amplification (HDA),^{36,37} strand displacement amplification (SDA),³⁸ loop-mediated isothermal amplification (LAMP),³⁹⁻⁴³ recombinase polymerase amplification (RPA).^{44,45} However, all target amplification strategies are sensitive to cross-contaminations, which produces false-positives, and, therefore, require trained personal and clean laboratory space.



Scheme 1. Classification of hybridization-based techniques for nucleic acid detection.

In probe amplification strategies, the amount of the target remains the same, but the probe sequence is replicated. One example of such techniques is rolling circle amplification (RCA),⁴⁶⁻⁵⁰ which was inspired by the mechanism of replication of viral circular DNA. In its linear amplification format, it allows approximately 1000-fold signal increase. RCA uses a padlock probe, which is a 5'-phosphorylated single-stranded DNA. The terminal fragments of the padlock probe are designed to be complementary to a target DNA or RNA. When the target is present, it brings together the terminal fragments of the probe, which forms a nicked circle being sealed by DNA ligase. The circularized padlock probe is then amplified using a DNA polymerase with strong strand displacement activity and no 5'-3'-exonuclease activity. As a result, long DNA molecule containing multiple repeats of the complementary sequence to the padlock probe is generated. This molecule can be detected by a conventional hybridization probe targeting the tandem repeat sequence.

Another technique to improve the LOD is to use chemical approaches to amplify the signal triggered by the presence of a target rather than the sequence of the target itself (signal amplification techniques in Scheme 1). The signal amplification techniques are rather heterogeneous. The examples of signal amplification approaches are branched DNA (bdNA) technology,^{51,52} hybridization chain reaction (HCR),⁵³⁻⁵⁵ tyramide signal amplification (TSA),⁵⁶ several liposome-assisted^{57,58} and nanomaterials-assisted strategies including bio-barcode⁵⁹⁻⁶¹ and dendrimer⁶² assays, among others. Some of these techniques have been extensively reviewed in literature.^{57,59,61,62-70}

A group of signal amplification strategies rely on target recycling to overcome the stoichiometric limitation of hybridization probes. In this approach, each target molecule initiates multiple signaling events. In enzyme-assisted target recycling (EATR) (Fig. 1A), the probe-target complex is specifically recognized by an enzyme (usually nuclease), and only the probe strand is cleaved. The cleaved probe generates a detectable signal. The two fragments of the cleaved probe have lower affinity to the target than the intact probe. This results in the target release for binding to another molecule of the probe and triggering its cleavage. Cycling of

hybridization and cleavage enables amplification of the signal. The advantages over target amplification strategies include less sensitivity to contamination and, as a result, less false positives due to linear rather than exponential character of amplification. In addition, most of the EATR assays are isothermal. Indeed, in target amplification approaches, the target is duplicated by elongation of a primer, and the resulting double-stranded DNA is too stable to dissociate without thermal denaturation. In contrast, specific cleavage of the probe in the target recycling approach would release the target without the need to increase the temperature.

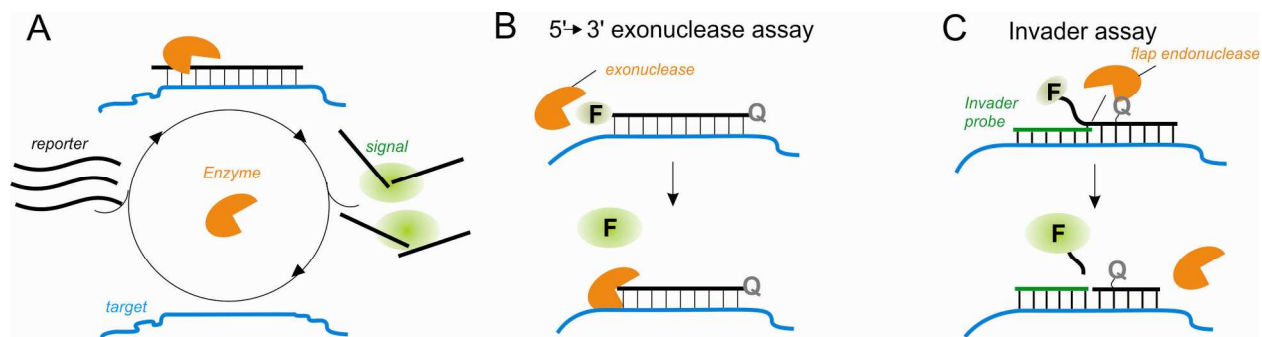


Fig. 1. Enzyme-assisted target recycling (EATR) for nucleic acid detection: a general strategy and two representative examples. (A) Generalized scheme of the approach. Target DNA binds a signal reporter oligonucleotide present in excess. The resultant reporter-analyte complex is processed by an enzyme, thus liberating the target. The reporter produces a signal after being cleaved. The released target molecule participates in the next round of signal production allowing signal accumulation. (B) The 5'→3' exonuclease assay.^{71,72} An oligonucleotide probe modified with a fluorophore and a quencher at its 5'- and 3'-ends, respectively, hybridizes to a specific nucleic acid analyte. DNA polymerase uses its 5'→3' exonuclease activity to hydrolyze the probe, thus releasing the fluorophore in solution. (C) Invader or flap endonuclease assay.⁷³⁻⁷⁵ A fluorophore- and quencher-labeled reporter probe forms a specific flap structure with the Invader probe and the target analyte. The structure is recognized by a flap endonuclease, which hydrolyzes the reporter and releases the fluorophore in solution, followed by fluorescence increase.

Two well-known mix-and-read EATR assays – the 5'→3' exonuclease assay and flap endonuclease assay – are illustrated in Figure 1B and C, respectively. In 5'→3' exonuclease assay, a fluorophore- and quencher-labeled probe is enzymatically cleaved upon hybridization to its target. This approach is commercialized in a real-time PCR format and known as Taqman assay. It takes advantage of the intrinsic 5'→3' exonuclease activity of DNA polymerases used for PCR.^{71,72} Flap endonuclease assay (Fig. 1C) is used for single nucleotide polymorphisms (SNP) genotyping and known as Invader assay.^{73,74} It can be used in a multiplex assay and allows detection of the target at the zeptomol (10^{-21} mol) level in a PCR-free format.⁷⁵ These two technologies have undoubtedly advanced nucleic acid analysis, and their success underlines the importance of EATR assays.

In this review, we focus on the most recent progress in the field of EATR-based nucleic acid detection. New variations of the approach achieve impressively low LOD, high specificity and selectivity, robustness and reduced cost. All these features are important for the point-of-care (POC) affordable diagnostics. The approaches are grouped based on nucleases used for the cleavage of the reporter substrates, which include restriction endonucleases, nicking endonuclease, exonuclease III, lambda exonuclease, RNase H and RNase HII, AP endonuclease, duplex-specific nuclease and DNase I.

2. Hybridization probes used for EATR

It is not an exaggeration to say that almost all variations of hybridization probes have been used with EATR strategy. The most commonly used probes/reporters are linear probes and hairpin probes (Fig. 2). Linear probes are short single-stranded oligonucleotides. For fluorescent detection a linear probe is labeled with a fluorophore, which can be an organic dye or a quantum dot (QD) (Fig. 2A). The probe can be additionally conjugated with a non-fluorescent quencher dye (Q) serving for reducing the fluorescence of the fluorophore in the intact probe. Such probe is commonly referred to as a dual-labeled probe, or a Taqman probe.^{76,77} When the probe is hybridized with a target, it is cleaved by an enzyme, which specifically recognizes the probe-target hybrid. Cleavage of the probe generates fluorescent signal. In some assays, nanomaterial, such as graphene oxide (GO), single wall carbon nanotubes (SWNT), carbon nitride nanosheets (CNNS) and Pd nanowires (NW), are used as quenchers. These nanomaterials demonstrate strong affinity to single-stranded DNA, while bind double-stranded DNA, mononucleotides and free fluorophores in much less extent.⁷⁸⁻⁸² This constitutes the basis for separation of the free probe from the probe-target complex. Hybridization to the target results in desorbing the complex from the nanomaterial surface in solution, where it is cleaved by an enzyme. Fluorophore-labeled fragments of the probe are accumulated in solution, resulting in high fluorescent signal.

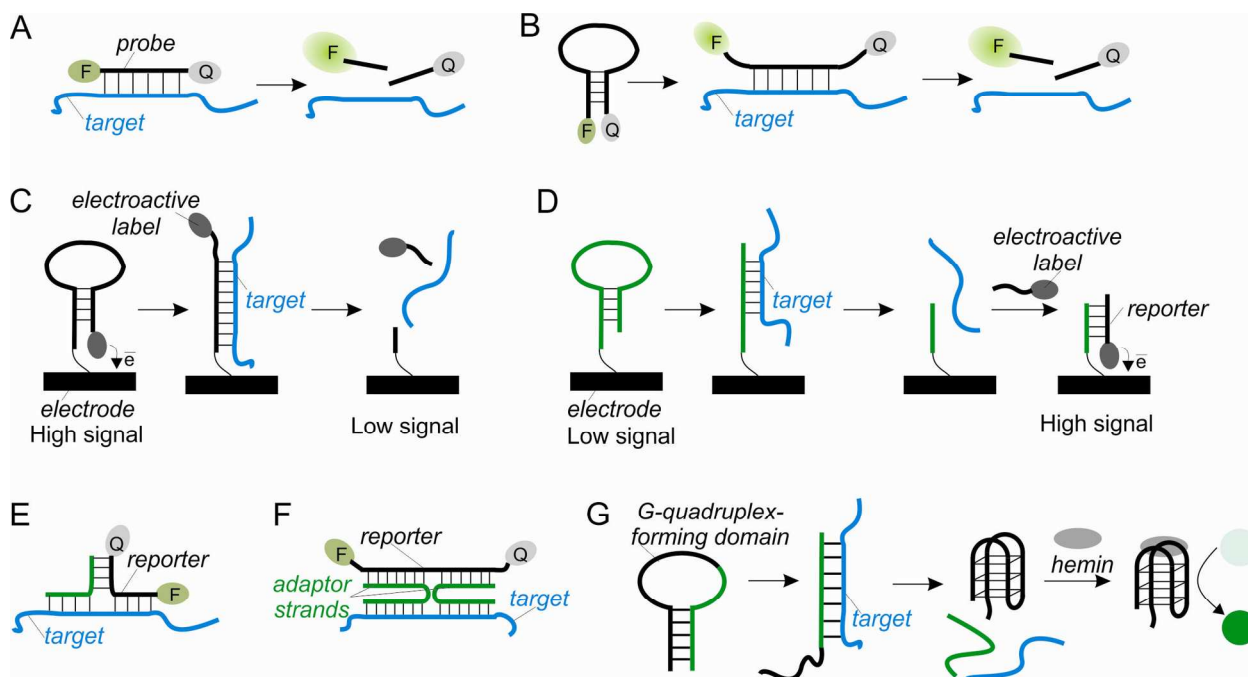


Fig. 2. Hybridization probes/signal reporters most commonly used in EATR. (A) Dual labeled or Taqman probe. (B) Molecular beacon (MB) probe. (C) Hairpin probe with electrochemical signal-OFF readout. (D) Hairpin probe with electrochemical signal-ON readout. (E) Three-way DNA junction (3J) probe. (F) Four-way DNA junction (4J) probe. (G) Probe containing a G-quadruplex-forming sequence.

Hairpin probes represent single-stranded oligonucleotides with complementary terminal fragments. In accordance with its name, a hairpin probe folds into a stem-loop structure (a hairpin). Molecular beacon (MB) probe is an example of hairpin probes with fluorescent readout (Fig. 2B).²²⁻²⁴ It contains a fluorophore and a quencher attached to the opposite ends of the

probe. The proximity of the fluorophore and quencher in the close MB conformation ensures low signal of the probe in the absence of the target. The target, which is usually complementary to the loop portion of MB probe, opens the hairpin and restores fluorescence. Enzymatic cleavage of the probe in the probe-target complex allows accumulation of the fluorescently label probe fragment and, therefore, amplifies the signal.

Electrochemical hairpin probe-based nucleic acid sensors can be realized in either signal-OFF or signal-ON format. Correspondingly, the signal either decreases or increases in response to the presence of the analyzed nucleic acid. Signal-on electrochemical sensors are not so susceptible to false positives and offer the advantage of improved LOD and dynamic ranges in comparison with signal-OFF sensors.⁸³ In a simple signal-OFF sensor, a hairpin probe immobilized on the electrode's surface is labeled with an electroactive tag, for example, methylene blue or ferrocene (Fig. 2C). The target-mediated cleavage of the probe results in the release of the label, which decreases the electrochemical signal. In a simple signal-ON design, the hairpin probe is unlabeled (Fig. 2D). It serves only for target recognition. The detection is realized through binding of a reporter, which is modified with an electroactive label, to a terminal fragment of the hairpin probe attached to the electrode. In the absence of the target, the hairpin probe cannot hybridize to the detector probe due to the strong stem. When the probe is cleaved by a nuclease upon binding to its complementary target, the electrode-immobilized fragment of the probe is left intact and, therefore, becomes available for hybridization with the reporter. This brings the electroactive label close to the electrode, thus increasing the signal (Fig. 2D). The aforementioned probes are examples of heterogeneous detection. Homogeneous electrochemical sensors, where the probe is not covalently attached to the electrode, have been also reported. In some designs, the electrochemical indicator is not covalently attached to the probe, but binds to the probe or probe-target complex from solution.

EATR strategy was also used with junction probes. These probes are made of several strands, which bind to their target nucleic acids forming three-way DNA junction (3J)⁸⁴ or four-way DNA junction (4J) structures⁸⁵ 3J probes, which are also called "Y-junction probes", contain two strands that are partially complementary to each other. In addition, both strands are complementary to the adjacent positions of the target. In case of fluorescent detection, one of the strands is labeled with a fluorophore/quencher pair and functions as a reporter (Fig. 2E). 4J probes consist of three strands, one of which is a reporter. Another two serve as adaptor strands by indirectly connecting the target to the reporter (Fig. 2F). The cleavage of the reporter destabilizes both 3J and 4J associates and results in releasing the target and fluorescent products in solution.

A number of EATR-based assays take advantage of G-quadruplex forming sequences as label-free signal reporters. It is known that in the presence of K^+ or NH_4^+ DNA with short G-rich repeats fold into the G-quadruplex structure,⁸⁶ which has strong affinity to porphyrins, such as hemin.⁸⁷ The complex of G-quadruplex with hemin acts as a peroxidase by catalyzing H_2O_2 -mediated oxidation of a number of organic compounds, which results in a color change or chemiluminescent signal.^{87,88} For nucleic acid detection purposes, the G-quadruplex-forming sequence is partially sequestered in the stem of a hairpin probe and, therefore, inactive in the absence of the target (Fig. 2G). Target-mediated cleavage of the probe releases the active G-quadruplex sequence. Addition of hemin, hydrogen peroxide and an organic substrate initiates the peroxidase reaction. One of the most commonly used peroxidase substrate is 2,2'-azino-bis(3-ethylbenzothiazoline-6-sulphonic acid) (ABTS). Its oxidation results in the green color of the solution that can be detected by the naked eye or using a colorimeter. Another substrate is

luminol, whose oxidation generates chemiluminescent signal. Alternatively, G-quadruplexes can bind a fluorescent porphyrin *N*-methyl mesoporphyrin (NMM) and thereby increase its fluorescence.

In the following sections of the review we will refer to Figure 2, to shorten the description of EATR approaches that use the standard probes.

3. EATR assays based on sequence-specific enzymes

The first group includes nicking endonucleases (NEases) and restriction endonucleases (REases). *Both endonucleases require a specific nucleotide sequence for recognition and cleavage. This may impose a limitation on the target sequence.*

3.1. Restriction endonuclease-assisted assays

REases recognize a short specific sequence of nucleotides (recognition site) in the double-stranded DNA and catalyze cleavage of phosphodiester bonds of the two strands within the sequence. The cleavage occurs in a fixed position inside or near the recognition site. They are naturally found in prokaryotes, where they serve to defend bacteria from phage invasion. A great variety of restriction endonucleases of different specificity is commercially available.

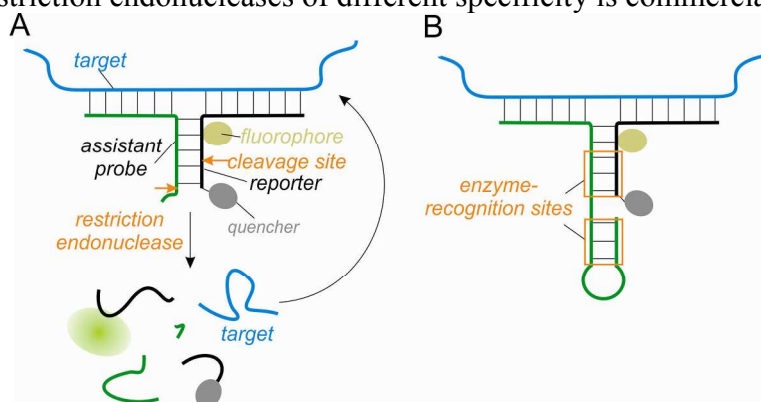


Fig. 3. Restriction endonuclease-assisted signal amplification with template enhanced hybridization processes (TeHyP) strategy for fluorescent nucleic acid detection. (A) Scheme for the assay with first generation 3J probes.⁸⁵ (B) Probe-target complex for the second generation 3J probes.^{94,95} Two enzyme-recognition sites increased the efficiency and decreased the time of the assay.

Since REases cleave both strands of the double-stranded DNA substrate, the use of REases for EATR with conventional probes will result in cleavage of the target along with the probe, thus target recycling would not be possible.⁸⁹⁻⁹³ To overcome this limitation, 3J probes are used. A group of Sintim suggested using 3J probes that operates via template enhanced hybridization processes (TeHyP).⁸⁵ In TeHyP strategy, one of the detection probes was labeled with a fluorophore and a quencher and, therefore, served as a signal reporter (Fig. 3A). A recognition site for *BfuCI* was in the probe-probe fragment between the attachment positions of the fluorophore and quencher. It was imperative to have at least one base pair between the probes junction and the enzyme recognition sequence, and attach the fluorophore group more than two nucleotides away from the recognition site. In addition, a 5'-overhang after the recognition site was required for enzymatic reaction to occur, so the blunt 5'-end at the unlabeled probe generated as a side product of *BfuCI*-catalyzed reaction inhibited the amplification cycle. A mismatch in the complementary region between the probes helped to reduce the background cleavage in the absence of the target. The approach offered excellent selectivity allowing

discrimination of single-nucleotide substitutions in the target sequence.⁸⁵ This high selectivity is the consequence of the semi-independent binding of the two probes to the target analyte and is shared by other binary probes.²¹

The strategy was adapted for RNA detection.⁹⁴ To reduce the undesired cleavage of the unlabeled probe, the authors introduced nuclease-resistant phosphothioate moieties into the cleavage site of the probe. In addition, a second nuclease-resistant enzyme-recognition site was introduced into the unlabeled probe in a form of stem-loop (Fig. 3B), which increased the efficiency of REase-catalyzed probe cleavage and considerably decreased the assay time to minutes (in comparison with several hours required in case of first probe generation). Such modification in the sensor design allowed detection of microRNA (miR-16), as well as *E. coli* 16S rRNA, both in total bacterial RNA preparation and in cell lysate. The modified assay was also applicable for SNP discrimination.

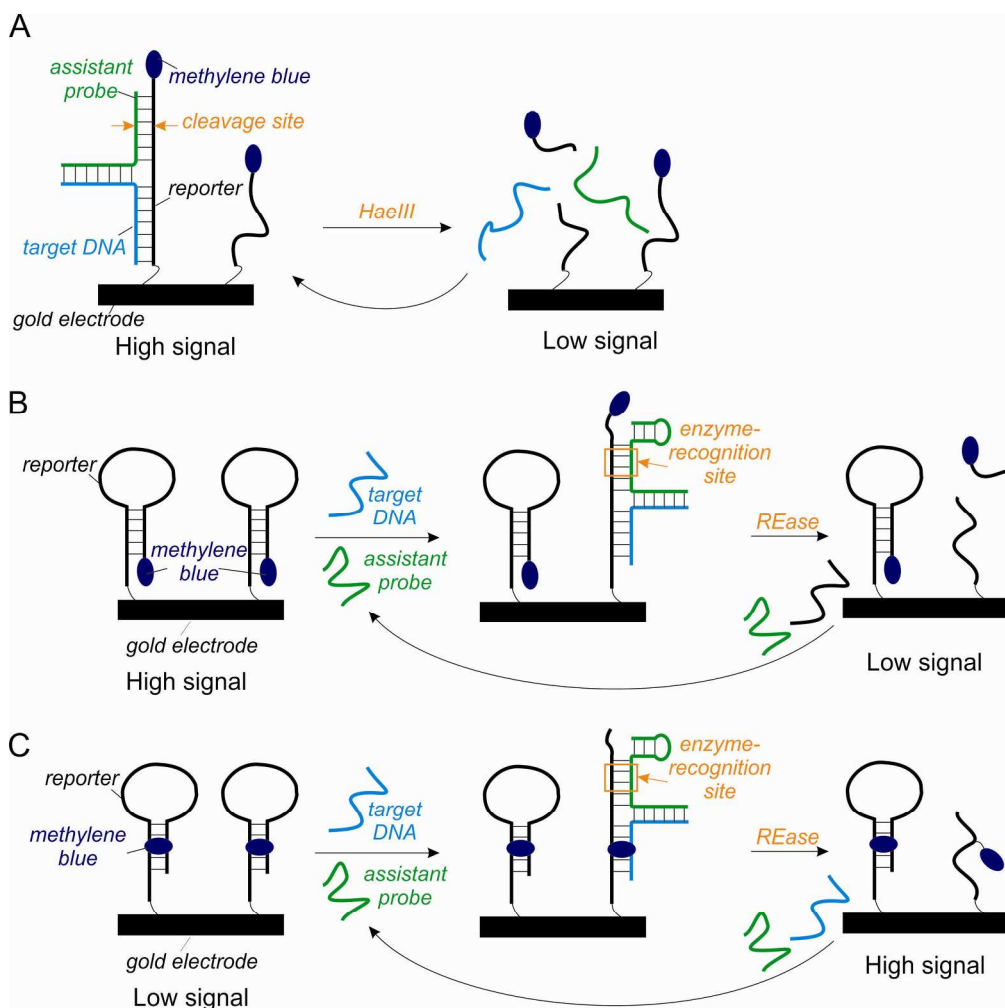


Fig. 4. REase-assisted electrochemical DNA detection using 3J probes. (A) A signal-OFF sensor using a linear methylene blue-labeled capture probe.⁹⁶ (B) A signal-OFF sensor made of a hairpin methylene blue-labeled probe.⁹⁷ (C) A signal-ON sensor made of a hairpin methylene blue-labeled probe.⁹⁷

A systematic study to identify REases suitable for the 3J probe-based EATR strategy revealed that only 12 REases out of 31 enzymes tested could be used with 3J probes – *BfuCI*,

FDSau3AI, *FDMoll*, *Bsp143I*, *Sau3AI*, *CfoI*, *CviQI*, *Csp6I*, *FDCsp6I*, *FDCsp6I*, *HaeIII*, *FDMspI*, *MseI* (FD standing for “fast digest” enzymes).⁹⁵ In addition, it was found out that in case of *Bsp143I*-aided assay the presence of a hairpin in one or both probes decreased the background cleavage in the absence of the target. However, this modification also reduced the fluorescence response in the presence of the target.

The REase-assisted 3J probes were also employed in combination with electrochemical signal output.^{96,97} In this case, either linear⁹⁶ (Fig. 4A) or hairpin⁹⁷ (Fig. 4B and C) probe/reporter containing methylene blue as an electroactive label were immobilized on a gold electrode. In the presence of the target DNA, the 3J structure was formed, and the enzyme cleaved the reporter into two fragments. In the signal-OFF format, the methylene blue-labeled cleavage fragment of the reporter was released into solution along with the target (Fig. 4A and B). As a result, the peak current decreased in a target concentration-dependent manner. A detection limit of 14 pM was reported for the signal-OFF sensor with the linear reporter.⁹⁶ The assay was able to differentiate between the target sequences differing in a single nucleotide. LOD of the hairpin capture probe (Fig. 4B) was ~1 nM.⁹⁷ In the signal-ON sensor design,⁹⁷ the methylene blue label was attached to an internal thymidine of the reporter and was intercalated into its double-stranded region, which decreased the probability of the label to approach the electrode. The reporter cleavage released the electro-active label on the single-stranded fragment followed by the increase in the electrochemical signal (Fig. 4C). The disadvantages of the approach were poor LOD (~1 nM) and long assay time. Interestingly, that out of six REases, most of which could work efficiently with 3J probes in a homogeneous format, only two enzymes – *Bsp143I* and *FDSau3AI* – were found to operate on solid support-bound 3J structures.⁹⁷

A biotin-labeled linear reporter was employed for photoelectrochemical DNA detection using indium tin oxide (ITO) coated with CdTe quantum dots-functionalized ZnO nanosheets as an electrode.* The signal was generated due to electrochemical reduction of H₂O₂ catalyzed by horseradish peroxidase-labeled reporter immobilized on the electrode's surface. In the presence of a target DNA, the capture probe along with an assistant probe, hybridized to the target forming a 3J structure with the recognition site for a restriction endonuclease *MboI* (similar to the approach depicted in Fig. 4). The enzyme cleaved off a short biotinylated fragment of the capture probe, thus decreasing the amount of horseradish peroxidase available for H₂O₂ reduction on the electrode surface. A detection limit of ~1 fM at a signal-to-noise ratio of 3 was achieved for a synthetic DNA target.

Another example of 3J probe-based electrochemical signal-OFF biosensor relied on competition between the cleaved and intact reporter for binding to an electrode-immobilized capture probe.⁹⁸ The unlabeled capture probe was complementary to the 3'-end of the 5'-biotinylated reporter. In the absence of the target, the reporter hybridized to the probe, thus resulting in labeling the electrode's surface with biotin. Biotin label attracted streptavidin-coated silver-nanoparticle-tagged carbon nanospheres (St-Ag-CNS), which generated high signal on the electrode (Fig. 5A). When target was present, a 3J structure containing *MboI*-recognition sequence was formed. The enzyme cleaved the reporter into two fragments, one of which preserved the biotin label, while another contained the sequence complementary to the capture probe. Since only the intact reporter probe could bring the biotin label to the electrode, the signal was low (Fig. 5B). The LOD of 66 aM was reported for a synthetic DNA target.

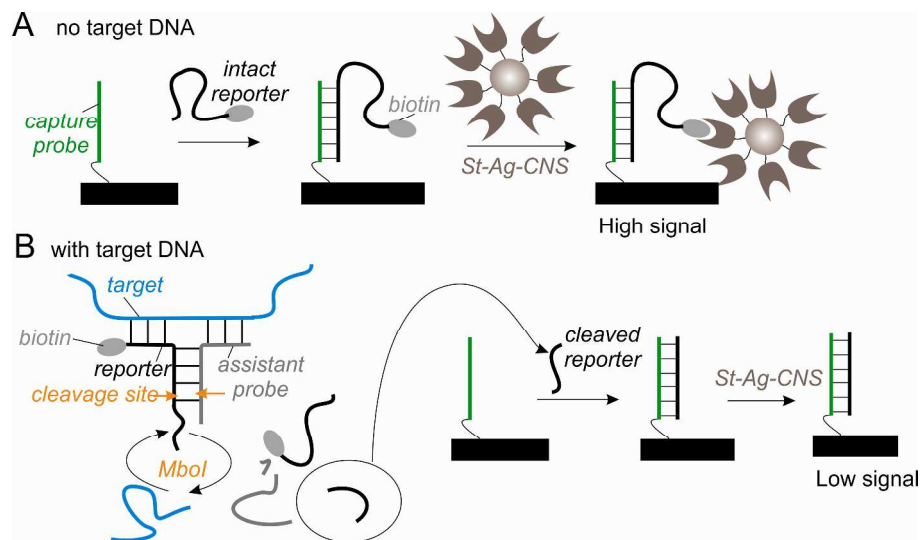


Fig. 5. Signal-OFF electrochemical sensor based on a competitive hybridization strategy.⁹⁸ (A) In the absence of the target, the intact reporter hybridized to the capture probe, which enabled high signal upon interaction with streptavidin-coated silver-nanoparticle-tagged carbon nanospheres (St-Ag-CNS). (B) The target-mediated cleavage of the reporter by *MboI* removed the biotin label, and the signal was low.

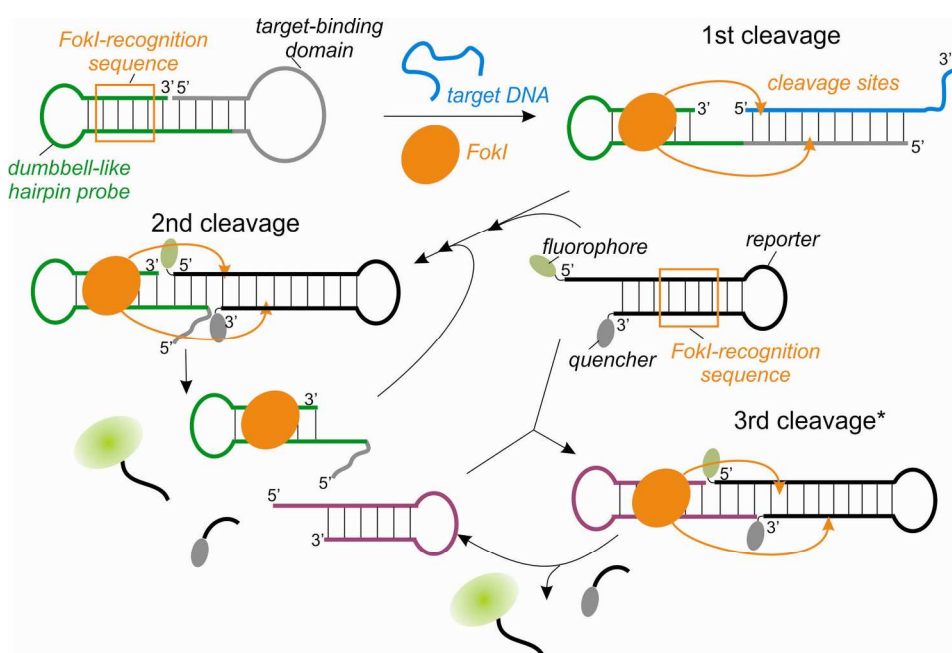


Fig. 6. Nucleic acid detection based on *FokI*-assisted signal amplification.⁹⁹ The original design contained only two cleavage events (1st and 2nd cleavage). For the third cleavage (*) event to occur, the reporter was modified to have another *FokI*-recognition sequence and self-complementary sequences.

An interesting design using a dumbbell probe and a hairpin reporter was developed by Willner and co-workers based on *FokI*/DNA scission machine.⁹⁹ *FokI* is a restriction endonuclease that cleaves two strands of the double-stranded DNA substrate 9 nucleotides downstream and 13 nucleotides upstream of the recognition site, respectively.¹⁰⁰ The assay utilized a dumbbell-shaped double-hairpin DNA structure containing the enzyme-recognition site

and a target-binding domain (Fig. 6). In the absence of the target DNA, *FokI* could bind to its recognition site but could not catalyze the cleavage, since the cleavage sites were missing. Upon hybridization of the dumbbell-shaped probe to the target, both the *FokI* recognition and cleavage sites were formed (Fig. 6, top). The cleavage fragment of the probe still containing the *FokI*-recognition sequence could form a complex with yet another hairpin DNA labeled with a fluorophore and a quencher at its opposite termini (reporter). Second *FokI*-catalyzed cleavage event resulted in separating the fluorophore from the quencher and restoring the fluorescent signal. This assay allowed detection of a Tay-Sachs genetic disorder mutant at as low as 100 pM level. To further amplify the signal, second *FokI*-recognition site was introduced into the reporter. In addition, it contained a self-complementary region, which enabled hybridization of the intact reporter with its hairpin fragment produced by the enzyme. Third scission event generated another molecule of the hairpin fragment, along with the fluorescent fragment. Hairpin fragments of both the dumbbell-like probe and the reporter were recycled in the system, thus amplifying the fluorescent signal. Such modification of the assay enabled improvement of the detection limit 10,000-fold down to 10 fM.

3.2. Nicking endonuclease-assisted assays

Similar to REases, nicking endonucleases recognize specific sequences in double-stranded DNA. Unlike REases, they introduce a cut into only one predetermined strand of the duplex producing a nick.¹⁰¹ Nowadays, nicking endonucleases of different specificity are commercially available. The majority of them are artificially engineered by altering restriction enzymes. Nicking enzymes seem to be more attractive for EATR signal amplification, since there are a lot more reports on NEase-depending assays than on the assays utilizing REases.

Since nicking endonucleases cut only one strand of the double-labeled DNA, it is possible to use a conventional linear probe complementary to an analyzed nucleic acid sequence in an NEase-assisted target-recycling format. Kiesling et al. introduced nicking endonuclease signal amplification (NESA) method for identification of specific single- or double-stranded DNA sequences.¹⁰² A linear reporter probe with a fluorophore label hybridized to a target DNA creating a recognition site for a nicking endonuclease followed by the reporter cleavage. The accumulated fluorescently labeled fragments of the probe were detected using capillary electrophoresis. The authors employed NESA for the detection of *Bacillus subtilis* and *Bacillus anthracis* genomic DNA. Cleavage of the probe catalyzed by *Nt.AlwI* was observed within one minute. Less than 30 CFU were sufficient to detect target present in a single copy per cell when NESA was used in combination with multiple displacement amplification of the genomic DNA. Moreover, the approach enabled differentiation of the targeted bacterial species from the closely related species.

A nicking endonuclease *Nt.BstNBI* was used for the detection of the hemmagglutinin gene of influenza virus, both in mix-and-read fluorescent and lateral-flow immunoassay formats.¹⁰³ In this approach a linear reporter was modified at the opposite ends either with a fluorophore/quencher pair (for mix-and-read assay) or with an antigen sulfamethoxydiazine and biotin (for a strip immunoassay). The enzyme cleaved the probe in the probe-target complex into two fragments, one of which carried either the fluorescent or antigen label for subsequent detection. Using the mix-and-read assay at 55 °C, $\sim 2 \times 10^{12}$ copies (~ 3.3 pM) of the target RNA were detected within 10-15 min. The authors also suggested a modified assay for the detection of the nucleic acid sequences that do not have endonuclease-recognition sites. In this modified assay, a validation probe was introduced. The probe contained a target-recognition fragment and

another fragment complementary to a universal reporter, whose sequence was target-independent. The enzyme recognized the duplex between the validation probe and reporter and cleaved the reporter into the detectable fragments. The intact complex between the target and validation probe could then bind another molecule of the reporter, thus enabling signal amplification. To separate the target from other nucleic acids present in the sample, a surface-immobilized capture probe complementary to another fragment of the target was required.

The NESAs approach was used with CdTe quantum dots (QDs) as fluorescent labels.¹⁰⁴ Magnetic beads served for capturing the QDs in the absence of the target. For this purpose, both magnetic beads and QDs were functionalized with short DNA oligonucleotides. A linear probe also served as a linker to connect the magnetic beads and QDs by hybridizing to the oligonucleotides attached to them. After separation from the beads, the solution fluorescence was low. When present, the target hybridized to the probe, thus forming the recognition sequence for a nicking endonuclease *Nt.AlwI* and enabling the probe cleavage. The probe could no longer link the QDs to the magnetic beads, and the fluorescence of the solution increased. As low as 5 fM of a synthetic DNA target could be detected by this approach. Unfortunately, the target must have the *Nt.AlwI*-recognition sequence to be analyzed by this approach. Alternatively, other endonucleases can be used, but only after re-optimization of the assay conditions. In addition, the assay required several steps of incubation at different temperatures.

A fluorescent NESAs assay was developed for the detection of 16S rRNA of a foodborne pathogen *Salmonella enteritidis*.¹⁰⁵ The assay made use of a linear probe containing a 9-nt terminal fragment complementary to a reporter (Fig. 7). The reporter was

labeled at its opposite ends with a carbon nanoparticle (CNP), which served as a fluorophore, and a Black Hole 1 as a quencher. The fluorescence of the intact reporter was low due to the proximity of the quencher to CNP. When no target was present, the probe was bound to carbon nanotubes (CNT) due to their affinity to single-stranded DNA. As a result, the probe was hidden from binding to the reporter. The target hybridized to the probe to form a probe-target duplex (Fig. 7), which resulted in breaking the connection between the probe and CNT due to

low affinity of CNT to the double-stranded DNA. As a result, the reporter could bind to the probe-target duplex and form a sequence recognized by *Nb.BbvCI*, which catalyzed cleavage of the reporter into two fragments. The cleaved reporter was released from the probe-target complex. Separation of the fluorophore from the quencher resulted in fluorescence increase. The LOD of 70 pM was demonstrated for a model single-stranded DNA analyte. When employed with lysate of *S. enteritidis*, the LOD was shown to be 100 CFU/mL. No signal above the background was detected in case of *S. typhimurium* or *E. coli*, proving high specificity of the assay.

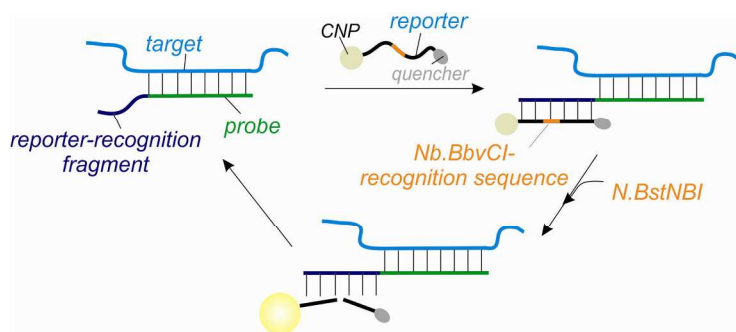


Fig. 7. CNT-based assay for *Salmonella enteritidis*.¹⁰⁵ Only in the presence of a complementary target the probe (Black and purple) could be desorbed from carbon nanotubes, which preferentially adsorb single-stranded DNA molecules. A reporter labeled with carbon nanoparticles (CNP) and a quencher hybridizes to the reporter-recognition fragment of the probe in the probe-target complex and forms the recognition sequence for *Nb.BbvCI*, which cleaves the reporter and restores the fluorescence of CNP.

The NESAs approach was used with an MB probe as a reporter.¹⁰⁶ The *N.Bst*NBI-recognition sequence was inserted in the loop portion of the MB probe. The enzyme cleaved the MB probe bound to the target, thus separating the fluorophore and the quencher. The reported detection limit of 6.2 pM was almost three orders of magnitude lower than that for a conventional MB assay without enzyme-assisted signal amplification. The assay was SNP-specific only when a mutation was either within the nicking endonuclease binding site or in the middle of the target fragment. Therefore, the high selectivity of the assay was attributed mostly to the disturbing effect of mutations on the enzyme binding.

An MB probe served as a reporter in a 3J-based NESAs assay.¹⁰⁷ In the presence of a target DNA, the MB probe could be opened due to the formation of a 3J structure containing the double-stranded *Nt.Bbv*CI-recognition site (Fig. 8). The enzyme then cleaved the MB probe producing fluorescent signal. The authors designed the probe to target a 23-nt fragment from the HIV-1 U5 long terminal repeat sequence. The optimized 3J probe could detect as low as 50 pM synthetic oligonucleotide target with the *Nt.Bbv*CI-mediated signal amplification, while without the enzyme the detection limit of only 1.6 nM was achieved. The probe was shown to be highly selective, with no signal above the background (the target-free reaction) produced in the presence of a single-base mismatched DNA target.

Similar 3J-based assay was employed for signal-OFF microRNA detection.¹⁰⁸ The assay used label-free mercury ion-mediated conformational MB as a signaling probe. The probe contained oligothymidylate terminal fragments that bound to each other due to the interaction of thymines via Hg^{2+} ions. When bound to the MB probe, mercury ions were unable to quench fluorescence of silver nanoclusters present in the sample, and the signal was high. In the presence of a microRNA target, the MB probe opened up due to the formation of the 3J structure. Released into solution, mercury ions quenched fluorescent signal of silver nanoclusters. The more MB probe molecules were opened by the released target, the more Hg^{2+} became available for fluorescence quenching. Such approach allowed detection of as low as 0.6 fM microRNA and discrimination of the target from a single-base mismatched microRNA.

In some of the EATR-based assays, dual amplification approach was employed to further improve the detection limit. For this purpose, methods for probe amplification, such as RCA, or even target amplification (e.g. SDA) were used. In such dual amplification strategies, the target functioned as a template for DNA ligase (in RCA) or as a primer for amplification of the probe sequence (in both RCA and SDA). Since the target triggered enzyme-catalyzed probe cleavage and was “reusable”, these approaches can still be referred to as a variation of EATR.

One example of dual amplification strategy relied on RCA to improve the LOD of the MB probe-based NESAs approach.¹⁰⁶ In this design the assay additionally used DNA padlock probe, DNA ligase, DNA polymerase and a primer (Fig. 9). Since a fragment of the padlock probe was complementary to the MB probe, the RCA single-stranded DNA product could bind many copies of the MB probe and, correspondingly, form many sites for the NEase recognition. As a result, the LOD of the assay was ~85 fM, which is a ~100-fold improvement over the RCA-based MB assay without the NESAs. The selectivity of the RCA-dependent assay was attributed to the mutation-tolerance of a DNA ligase, since the target interacted directly only with the padlock

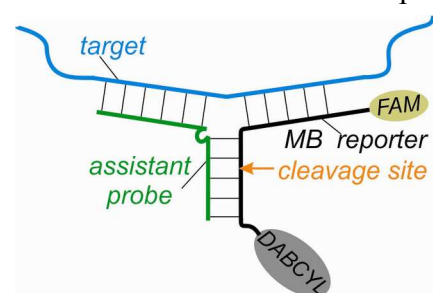


Fig. 8. 3J structure formed between the target, assistant probe and MB probe.¹⁰⁷ The site of MB probe cleavage by *Nt.Bbv*CI is shown with an arrow.

probe. Indeed, T4 DNA ligase was sensitive only to a mutation next to the nick site in the probe, while *E. coli* DNA ligase allowed discrimination of all mutations around the nick site.

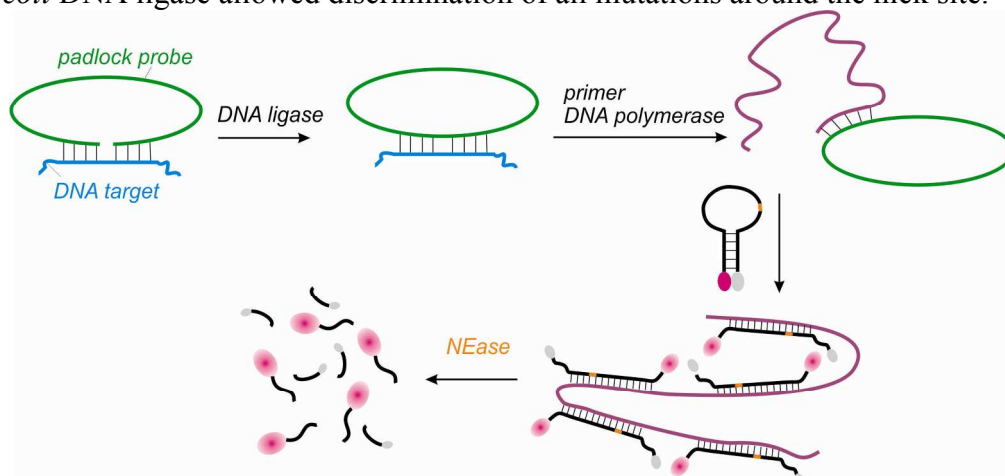


Fig. 9. RCA-dependent NEase-assisted signal amplification (NESA) with an MB probe as a reporter.¹⁰⁶

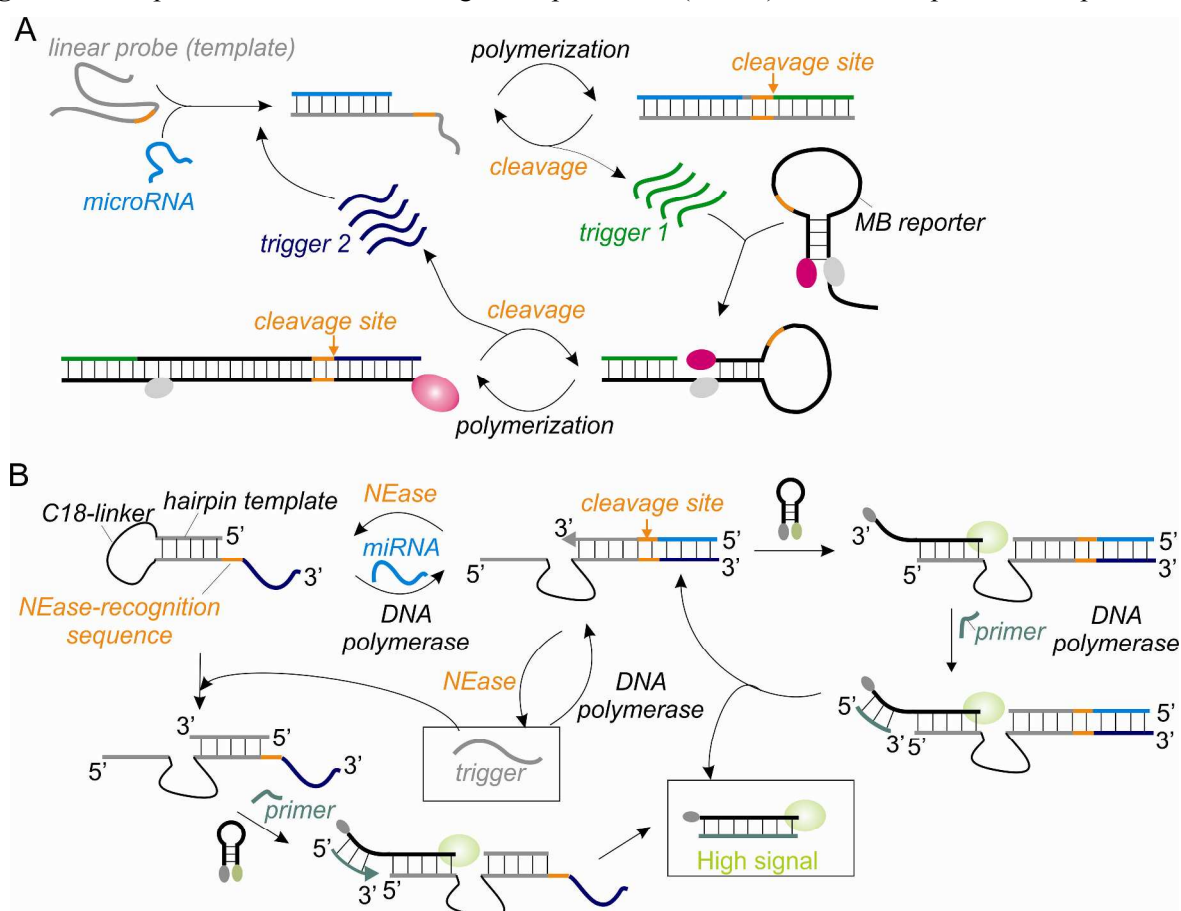


Fig. 10. Fluorescent exponential amplification assay for microRNA based on the combination of NESA and SDA. An NEase-recognition sequence is shown in orange, with the orange arrow pointing at a cleavage site. (A) Linear template-based assay.¹⁰⁹ (B) Hairpin template-based assay.¹¹¹

NESA/SDA dual amplification strategy with fluorescent readout was described for microRNAs detection.¹⁰⁹ A microRNA target hybridized to a linear probe and served as a primer for a DNA polymerase, which extended the microRNA and formed a double-stranded

polymerization product containing the recognition sequence for a nicking enzyme *Nt.BstNBI* (Fig. 10A). The enzyme cleaved the newly synthesized strand of the product releasing the universal trigger 1. This sequence was complementary to the 3'-terminal single-stranded fragment of an MB probe served as a reporter. The MB probe contained a fluorophore at its 5'-end and a quencher at an internal nucleotide across from the fluorophore in the stem. In addition, the reporter contained the *Nt.BstNBI*-recognition sequence in its loop portion. In the closed conformation, the fluorescence of the reporter was quenched. Hybridization of the trigger to the reporter resulted in the trigger elongation by the second SDA reaction, which opened the hairpin and restored its fluorescence. Due to the formation of another double-stranded recognition sequence, the nicking enzyme cleaved the fluorescent double-stranded polymerization product, releasing trigger 2. The sequence of trigger 2 corresponded to that of the target microRNA. Therefore, it could serve as a primer for the first SDA reaction. Two SDA and two nicking reactions working together resulted in exponential amplification of the signal by converting one target molecule into numerous trigger molecules. This dual strategy allowed a detection limit of 0.38 pM with the ability to discriminate between microRNA differing in a single nucleotide. Similar assay utilizing a dual-labeled probe instead of the MB probe has been recently employed for the detection of methylated DNA.¹¹⁰ The detection limit of 0.78 pM was achieved, and as low as 0.1% methylation level was shown to be distinguished from the mixture of methylated and unmethylated DNA.

Another SDA/NESA-based assay for microRNA analysis made use of a hairpin template containing a 3'-overhang fragment complementary to the target microRNA adjacent to the specific *Nt.BsmAI*-recognition sequence (Fig. 10B).¹¹¹ The stem-forming fragments were joined by an 18-carbon spacer. The target was elongated by DNA polymerase followed by the *Nt.BsmAI*-catalyzed cleavage of the newly synthesized strand to regenerate the target and produce a DNA trigger, whose sequence was complementary to the stem region of the template. Both elongation of microRNA and binding of the DNA trigger opened the template, thus initiating the template recognition by an MB probe. The 3'-terminal fragment of the MB probe was complementary to an external primer, which was elongated by DNA polymerase to produce a fluorescent double-stranded complex of the MB probe with its complement (high signal). The cycling of these reactions resulted in the cascaded amplification of the fluorescent reporter resulting in LOD of 1 fM. The assay was able to differentiate between the members of the same microRNA family.

To achieve low detection limits, cascade enzymatic signal amplification (CESA) approach was suggested.¹¹² The approach combined the following three components: *Afu* flap endonuclease-based invasive signal amplification, flap ligation and NESA (Fig. 11). First step was based on the Invader assay and involved two probes – a downstream probe (dp) and upstream probe (up). When up and dp hybridized to the target, dp formed a 5'-flap that was cleaved off by *Afu* flap endonuclease (Fig. 1C). This resulted in release of the target-complementary dp fragment into solution and triggered binding of another intact dp to the up-target complex (Fig. 11A). As a result, one target molecule could generate several thousand cleaved flaps. Second step required ligation of the flap with a 5'-phosphorylated oligonucleotide (p-oligo) using an MB probe as a ligation template. The flap and p-oligo hybridized to the adjacent positions of the loop fragment of the MB probe and, upon ligation, opened up the probe increasing fluorescence (Fig. 11B). The fluorescent signal was then amplified using the NESA approach. The complex between the MB and the ligated flap contained a recognition sequence for *Nt.BsmI*, which cleaved the MB into two fragments. Cleavage resulted in release and spatial

separation of the fluorophore- and quencher-containing MB fragments (Fig. 11C). One ligated flap molecule could initiate cleavage of multiple copies of the MB probe. Working together, the two EATR strategies (flap endonuclease assay and NESAs) enabled exponential signal amplification and enabled detection of 1 fM target.

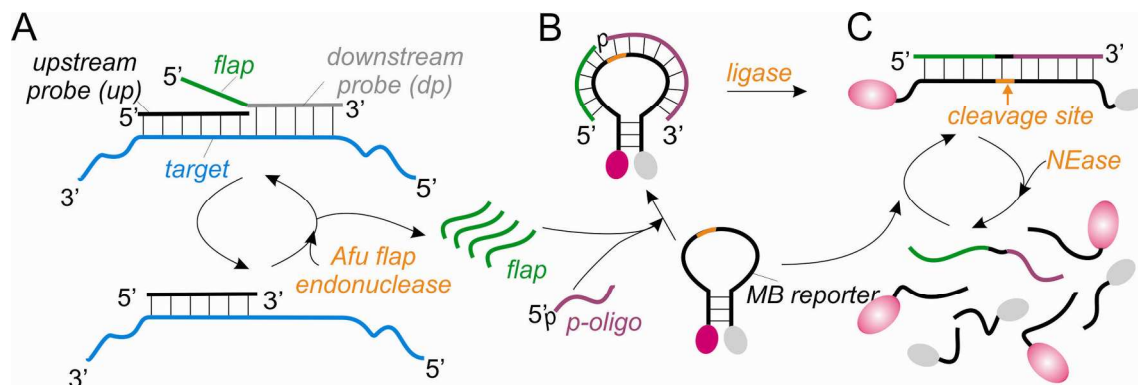


Fig. 11. Cascade enzymatic signal amplification (CESA) approach.¹¹² (A) A downstream (dp) and an upstream probe (up) bind to a nucleic acid target forming a complex with a 5'-flap, which is cleaved off by *Afu* flap endonuclease. (B) The cleaved flap binds to an MB reporter adjacent to a 5'-phosphorylated oligonucleotide (p-oligo), and a DNA ligase ligates the two oligonucleotides, which opens up the reporter. (C) The complex between the ligated flap and the reporter contains a sequence recognized by a nicking endonuclease, which cleaves the reporter amplifying the fluorescent signal.

A number of studies aimed at visual/colorimetric detection of nucleic acid targets. NESAs-based assays with visual or colorimetric readout are promising for instrument-free nucleic acid analysis. For this purpose, several research groups suggested using a horseradish peroxidase-mimicking deoxyribozyme, (Fig. 2G). Similar colorimetric DNA detection assays using the basic NESAs approach were independently reported by two research groups.^{113,114} In both works, the G-quadruplex structure was sequestered with an 8-nucleotide long stem in a hairpin probe, which opened up upon hybridization to a DNA target (Fig. 12, left). The target-probe duplex carried the *Nt.BstNBI*-recognition site, and the enzyme cleaved the probe, releasing the active peroxidase deoxyribozyme into solution. When hemin, ABTS and H₂O₂ were added, the solution turned green indicating the presence of the DNA target (Fig. 12, right). The intact target triggered multiple rounds of the peroxidase activation, thus amplifying the signal. This signal amplification strategy allowed the LOD of 1 pM¹¹³ or 10 pM¹¹⁴ depending on the structure of the hairpin probe and the assay conditions. These values of the LOD are 3-4 orders of magnitude lower than for similar colorimetric assays without signal amplification.^{21,114-116} High selectivity of the assay owing to the specificity of *Nt.BstNBI* recognition allowed differentiation between the fully complementary and a single nucleotide mismatch targets.

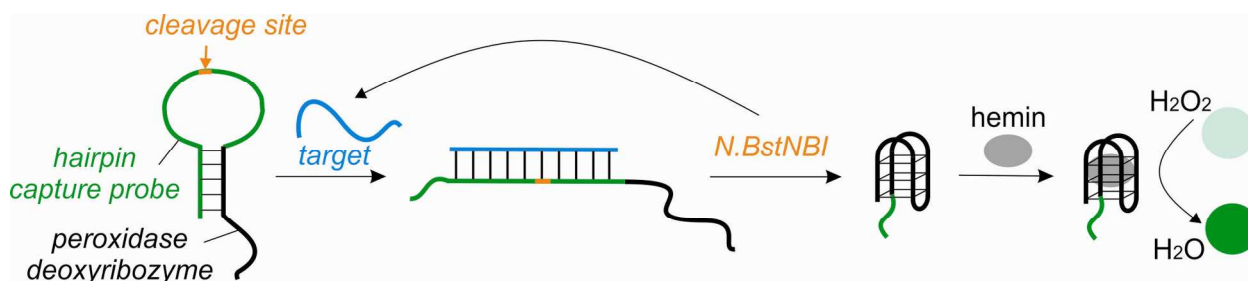


Fig. 12. Colorimetric assays using the basic NESAs approach.^{113,114}

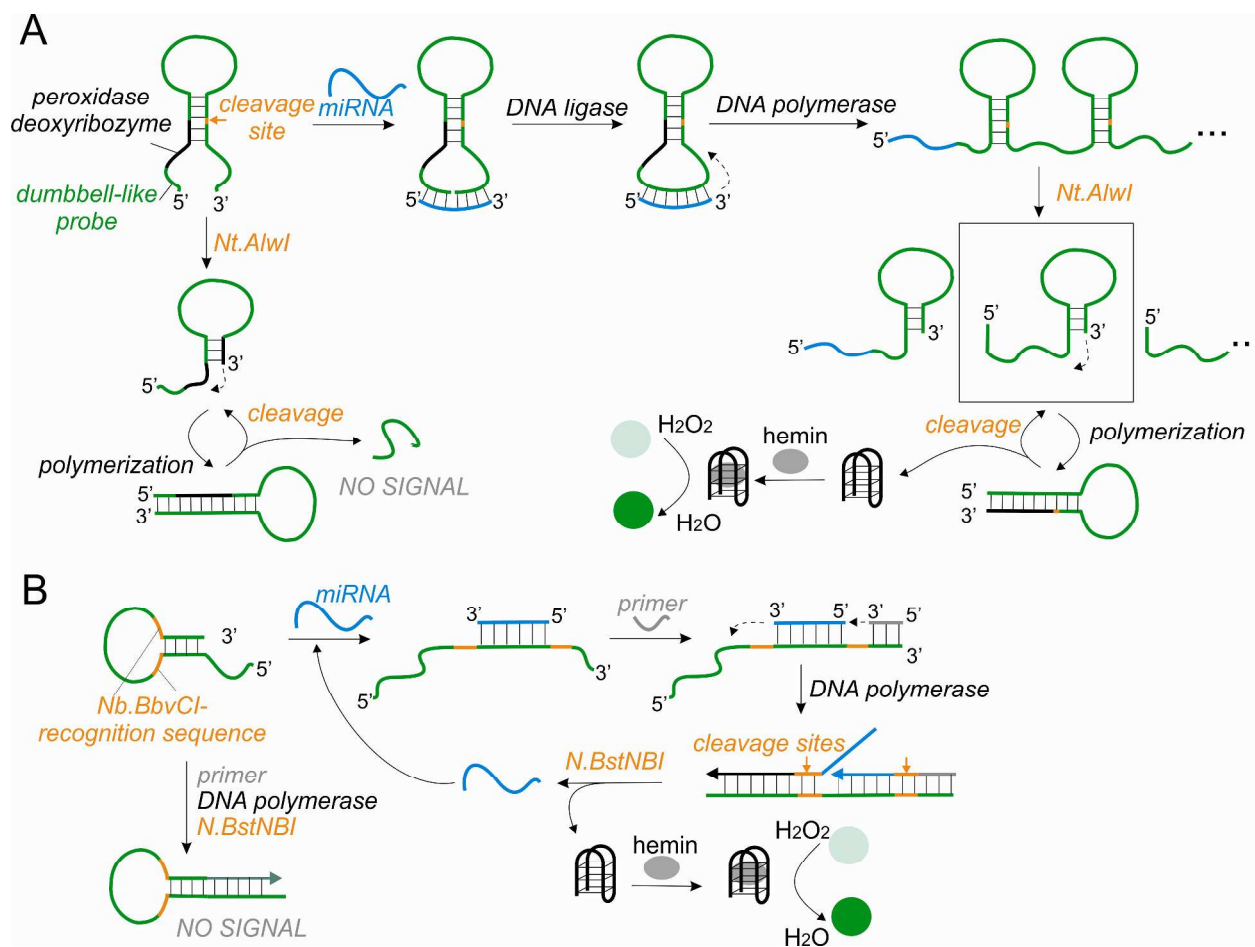


Fig. 13. Colorimetric assays for microRNA detection based on dual amplification strategy. (A) Rolling circle amplification (RCA)-dependent approach.¹¹⁷ (B) Strand displacement amplification (SDA)-dependent approach.¹¹⁸

Several colorimetric assays utilizing dual amplification strategy were described. The NESA approach was combined with either RCA¹¹⁷ or SDA¹¹⁸ to enable colorimetric detection of microRNA (Fig. 13). In one report, a cascade amplified assay utilizing a dumbbell-like probe consisting of a stem, loop and a mimic-loop was suggested (Fig. 13A).¹¹⁷ The sequence of peroxidase deoxyribozyme was partially caged in the stem. A microRNA target hybridized to the terminal fragments of the mimic-loop serving as a template for the ligation of the two ends and producing a circularized dumbbell structure. Then, the microRNA target served as a primer in RCA reaction, which generated a long single-stranded DNA product containing multiple repeats complementary to the peroxidase deoxyribozyme sequence. The recognition sequence for a nicking endonuclease *Nt.AlwI* was in the stem fragment of the dumbbell probe and, consequently, of the RCA product. Upon the NEase cleavage, the polymerase-induced replication was initiated, which displaced the nicked strand. As a result of continuous nicking, polymerization and displacement, multiple copies of single-stranded DNA fragments containing the peroxidase deoxyribozyme sequence were produced. In the presence of hemin, these active deoxyribozymes catalyzed H₂O₂-dependent oxidation of ABTS generating a visual signal. In the absence of the target microRNA, the NEase could cleave the dumbbell-like probe. However, the fragment contained complementary sequence of the peroxidase deoxyribozyme incapable of

catalysis (Fig. 13A, bottom left). The LOD of 50 aM (1 zmol in a 20- μ L sample) was achieved. The assay discriminated closely related sequences from the same microRNA family.

When NESAs were used in combination with SDA, a microRNA target opened up a hairpin probe containing the single-stranded 5'-terminal fragment complementary to the peroxidase deoxyribozyme (Fig. 13B).¹¹⁸ The target then served as a primer for DNA amplification. An additional primer complementary to the 3'-terminal fragment of the probe was employed. In the presence of a DNA polymerase and dNTPs, double-stranded structures, which contained two recognition sites for a nicking endonuclease *N.BstNBI*, were synthesized. The nicking enzyme cleaved the newly-synthesized strand releasing the fragments containing either the peroxidase deoxyribozyme or the target. The target could initiate next round of polymerization/cleavage. The peroxidase ribozyme bound hemin and catalyzed ABTS oxidation to produce green color. In the absence of the microRNA, no signal could be generated, since the newly synthesized strand for peroxidase deoxyribozyme was blocked in the stem (Fig. 13B, left bottom). The detection limit of 0.5 fM was reported.¹¹⁸

The basic NESAs approach was employed to fabricate electrochemical DNA sensors.^{119,120} A hairpin capture probe contained a 5'-terminal thiol group for the probe anchoring on the surface of a gold electrode (Fig. 2C and D). The loop portion of the hairpin probe was complementary to a DNA target. Upon hybridization to the target the hairpin probe opened up, and a double-stranded recognition sequence for a nicking endonuclease *N.BstNBI* was formed in the target-probe complex. The enzyme cleaved the hairpin probe followed by the target release, which enabled signal amplification. The sensor could operate in a signal-OFF¹¹⁹ or signal-ON¹²⁰ formats. In a signal-OFF format, the high signal in the absence of the target was attributed to the proximity of a ferrocene tag at the 3'-terminus of the hairpin probe to the electrode's surface. In the presence of the target, the tag-containing fragment of the probe was cleaved off, and the signal decreased (Fig. 2C). In case of the signal-ON sensor, a 3'-ferrocene-labeled reporter was used. It was complementary to the portion of the hairpin probe that remained attached to the electrode upon the *N.BstNBI*-catalyzed probe cleavage (Fig. 2D). Both sensors demonstrated low detection limits and high selectivity.

Another electrochemical sensor made use of a dual amplification strategy based on the combination of the NESAs and super-sandwich DNA self-assembling approaches (Fig. 14).¹²¹ In this strategy, multiple copies of a biotinylated hairpin capture probe 1 (CP1) were attached to the streptavidin-coated magnetic beads via streptavidin-biotin interactions. The CP1 had a target-recognition fragment with the *N.BstNBI*-cleavage site. In the presence of the target, the CP1-target hybrid was formed and recognized as a substrate by the NEase, which cleaved the CP1 and released the target and one of the CP1 fragments in solution (Fig. 14A). The latter served as an intermediate DNA. It contained a fragment complementary to the second capture probe, CP2, which was immobilized on a gold electrode (Fig. 14B, left). Another fragment of the intermediate DNA was complementary to a portion of the first helper probe, which, in turn, was complementary to the second helper probe. Upon hybridization of CP2, intermediate DNA and both helper probes, a supersandwich was assembled on the electrode's surface (Fig. 14B, middle). This assembly electrostatically adsorbed multiple copies of a positively charged $[\text{Ru}(\text{NH}_3)_6]^{3+}$ (RuHex) indicator, which produces electrochemical signal (Fig. 14B, right). This integrated strategy allowed the LOD of 0.36 fM and differentiation of the target from excess of non-complementary or single base-mismatch DNA sequences. An important limitation of this strategy is that target sequences must contain the enzyme-recognition site.

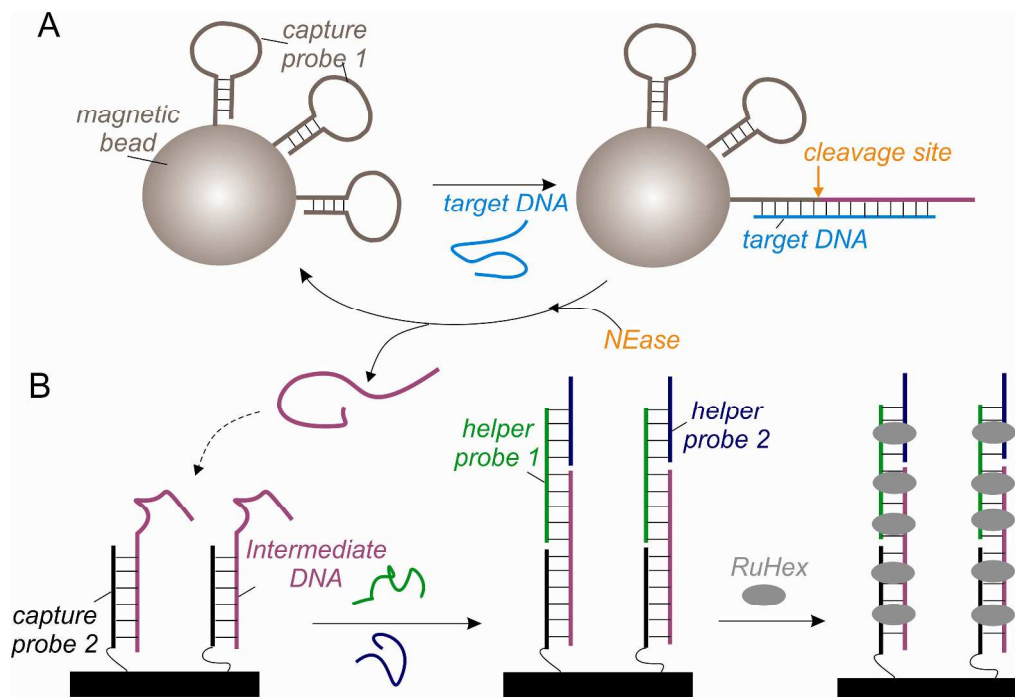


Fig. 14. Dual signal amplification strategy based on the NESAs and supersandwich assemblies for electrochemical DNA detection.¹²¹ (A) A DNA target binds to a hairpin capture probe attached to magnetic beads, thus forming a NEase recognition sequence. The enzyme cleaves the capture probe releasing an intermediate DNA and the target in solution. (B) The intermediate DNA hybridizes to a linear capture probe immobilized on a gold electrode and, together with two helper probes, forms a supersandwich associate, which adsorbs a RuHex electrochemical indicator.

A hairpin probe immobilized on a glassy carbon electrode coated with the K-doped graphene-CdS:Eu nanocrystal (K-GR-NC) composite film was used to design an electrochemiluminescence (ECL) signal-OFF DNA biosensor.¹²² K-GR-NC served for improving the intensity of the ECL signal and provided a large specific surface for DNA loading. The stem portion of the hairpin probe sequestered a G-quadruplex-forming sequence. When the loop portion of the probe hybridized to the target, the recognition sequence for *Nt.AflwI* was formed. The enzyme cleaved the probe enabling the electrode-immobilized G-rich fragment to fold into the active G-quadruplex, which bound hemin and electrocatalyzed the reduction of H_2O_2 decreasing the ECL signal. There was linear relation between the ECL decrement and the logarithm of target concentration in the range of 50 aM-10 pM with the LOD of 50 aM. The sensor could differentiate between one-base mismatched sequences. Interestingly, a chemiluminescent assay using Fe_3O_4 -Au nanoparticles enabled the LOD of ~ 0.86 fM.¹²³ Even lower LOD of 20 aM was achieved for another G-quadruplex-based sensor with ECL readout for the detection of DNA species related to oral cancer markers.¹²⁴

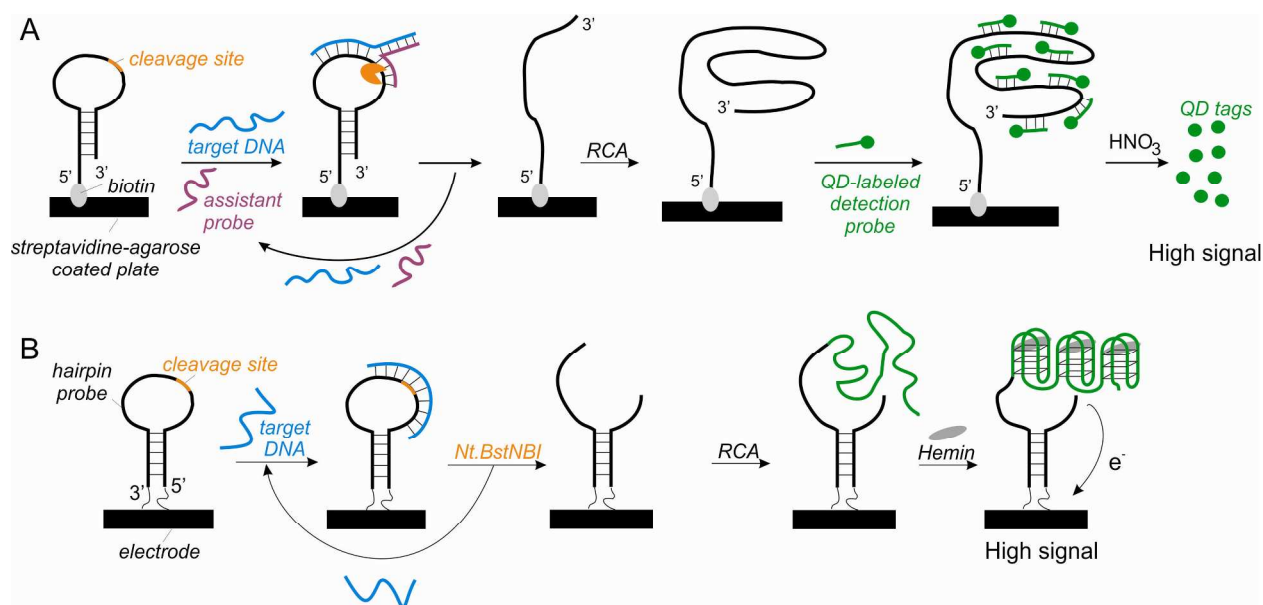


Fig. 15. Dual amplification strategy based on NESAs and RCA utilizing hairpin probes for electrochemical DNA detection. (A) Cascade signal amplification with QD-labeled detection probe.¹²² (B) G-quadruplex-dependent assay.¹²³

Dual amplification strategy combining NESAs with RCA using electrode-immobilized hairpin probes was reported.^{125,126} In one assay, the biotin-labeled probe was attached to the streptavidin agarose coated plate (Fig. 15A).¹²⁵ Together with an assistant probe from solution, it hybridized to a target DNA forming a 3J structure that contained the specific cleavage site for nicking endonuclease *Nt.BbvCI*. Enzymatic cleavage of the probe destabilized the 3J structure, and both the target and the assistant probe were released to amplify the amount of the cleaved hairpin probes. The hairpin probe fragment attached to the solid surface of the plate served as a primer for the RCA reaction using an external circular template. The product of RCA contained multiple copies of a repeated oligonucleotide sequence recognized by the CdTe QD-labeled detection probe. Finally, the cadmium component of QD-tagged RCA product was dissolved in HNO₃ to be quantified by the stripping voltammetric analysis. By employing this four-step analysis, it was possible to detect as low as 0.55 zmol of a DNA analyte in a 50 μ L sample, which corresponds to 11 aM DNA. Remarkably, the dynamic range was shown to be 6 orders of magnitude, from 10 aM to 10 pM. It is interesting that without RCA the assay was also quite sensitive: a detection limit of about 10 fM was achieved.¹²⁵ In another assay, a double-stranded probe-target complex was formed (Fig. 15B).¹²⁶ Enzymatic cleavage of the probe produced an electrode-immobilized fragment that could serve as a template for ligation of an external padlock probe and as a primer for subsequent RCA. The padlock probe encoded a G-quadruplex-forming sequence possessing affinity to hemin. Therefore, multiple G-quadruplex motives were formed. Their interaction with hemin provided a means for direct electron transfer between hemin and the electrode. The LOD of 0.25 fM was achieved with a synthetic DNA target mimicking the mutant human p53 gene.

In conclusion, the NESAs approach was employed either alone or in combination with the Invader or probe amplification approaches to develop a number of nucleic acid sensors with fluorescent, colorimetric or electrochemical readouts. The lowest LOD was achieved when the NESAs strategy was combined with another amplification strategy (Table 1). It is interesting to

note that even without additional amplification the LOD in the attomolar range was achieved for a chemiluminescent biosensor.¹²²

NESA assay was applied in colorimetric/visual format using gold nanoparticle assembling/disassembling.¹²⁷ The detection limit of 10 pM was reported. This assay might be especially useful for point-of-care detection of point mutations.

Table 1. The LOD for the reported NESA-based assays.^a

NEase	Recognition and cleavage site	Signal readout	Probe	LOD	Ref.
Nt.AlwI	5'-GGATCNNNN ⁺ N-3' 3'-CCTAGNNNN N -5'	F/CE	LP	30 CFU of <i>Bacillus subtilis</i> and <i>Bacillus anthracis</i>	102
		F	LP/magnetic beads	≤5 fM	104
		C	DP/RCA	50 aM	117
			LP/GNP	~10 pM	127
		ECL	HP	50 aM	122
		CL	HP	~0.86 fM	123
Nt.BstNBI	5'-GAGTCNNNN ⁺ N-3' 3'-CTCAGNNNN N -5'	F	LP	~2x10 ¹² copies of influenza virus hemmagglutinin gene	103
			MB	6.2 pM; ~85 fM (with RCA)	106
			LP/SDA/HP reporter	380 fM	109
		EC	HP (signal-OFF)	68 aM	119
			HP (signal-ON)	167 fM	120
			HP/super-sandwich (signal-ON)	360 aM	121
			HP/RCA	250 aM	126
		C	HP	1 pM	113
				10 pM	114
		ECL	LP	20 aM	124
Nt.BbvCI	5'- CCTCA GC-3' 3'-GGAGT ₁ CG-5'	F	3JP	50 pM	107
				0.6 fM	108
			LP/SDA/ linear dual-labelled reporter	0.78 pM of methylated DNA	110
			LP/ CNT	70 pM; 100 CFU/ mL of <i>Salmonella enteritidis</i>	105
		EC	HP	10 fM; 11 aM (with RCA)	125
		C	HP/SDA	0.5 fM	118

Nb.BsmI	5'-GAATGC N-3' 3'-CTTACG ₁ N-5'	F	Invader/MB	1 fM	112
Nt.BsmAI	5'-GTCTCN ¹ N-3' 3'-CAGAGN N-5'	F	HP/SDA/ MB reporter	1 fM	111

^a**Signal readout:** F - fluorescent; C - colorimetric; EC - electrochemical; ECL - electrochemiluminescence. CE - capillary electrophoresis-assisted detection; CL - chemiluminescence. **Probe:** LP - linear probe; HP - hairpin probe; DP - dumbbell probe; MB - molecular beacon probe; 3JP - three-way junction (3J) probe. GNP - gold nanoparticles; CNT- carbon nanotube; RCA - rolling circle amplification; SDA - strand displacement amplification.

4. EATR assays based on sequence-independent enzymes.

The main disadvantage of NEases and REases as enzymes for EATR approaches is their sequence-specificity: both types of enzymes require specific nucleotide sequence to be present in the probe and its complementary target. It imposes the limitation on the target sequence. To overcome this limitation, the use of sequence-independent nucleases has been suggested. Examples of such enzymes include exonuclease III, λ exonuclease, RNases HI and HII, apurinic/apyrimidinic (AP) endonuclease, duplex-specific nuclease (DSN), DNase I, and T7 exonuclease (Table 2). These enzymes catalyze cleavage of phosphodiester bonds in either DNA or RNA. Although the abovementioned nucleases do not require specific recognition sequence in their substrate, they still display some substrate preference. For example, λ exonuclease needs a cleavable DNA strand to have a phosphate group on its 5'-end. AP endonuclease makes a cut at the 5' of an AP site. Most of abovementioned nucleases use double-stranded DNA or DNA/RNA hybrid as substrates, while DNase I, for example, is active on both single- and double-stranded DNA, as well as on DNA in DNA/RNA hybrids. Among the sequence-independent nucleases, exonuclease III seems to be more commonly used for EATR.

Table 2. The enzymes utilized in EATR assay.^a

Enzyme	Activity	Preferential substrate	Comments
Exonuclease III	3'→5' stepwise removal of dNMP	dsDNA with blunt of recessed 3'-end	dsDNA with 3'-protruding end of less than four nucleotides can be processed by the enzyme
Lambda exonuclease	5'→3' stepwise removal of dNMP	dsDNA with a 5'-phosphorylated end	non-phosphorylated dsDNA and ssDNA can be digested at a greatly reduced rate
RNase H	endonucleolytic RNA hydrolysis	RNA/DNA hybrids	if used on DNA-RNA-DNA/DNA chimeric substrate, the ribonucleotide insert should be at least four nucleotides
RNase HII	endonucleolytic RNA hydrolysis	RNA/DNA hybrids	preferentially nicks 5' to a ribonucleotide within dsDNA
AP endonuclease	incising the apurinic/apyrimidinic (AP) sites from DNA backbone	dsDNA with an AP site	It nicks the dsDNA at the phosphate groups 3' and 5' to the AP site. Depending on the class, AP endonucleases generate either 3'-OH/5'-phosphate or 3'-phosphate/5'-OH termini.

Duplex-specific nuclease	DNA cleavage	dsDNA and DNA/RNA hybrids	requires perfectly matched duplexes of 8-12 bp in length
DNase I	endonucleolytic DNA cleavage	ssDNA, dsDNA and DNA/RNA hybrids	produces di-, tri- and oligonucleotides with 5'-phosphates and 3'-OH groups
T7 exonuclease	5'→3' stepwise removal of dNMP	dsDNA and DNA/RNA hybrids	unable to degrade ssRNA or dsRNA

^adNMP – deoxyribonucleoside monophosphate; ds – double-stranded; ss – single stranded

4.1. Exonuclease III-assisted assays

Exonuclease III catalyzes the stepwise removal of mononucleotides in the direction from 3' to 5' terminus. The preferred substrate for the enzyme is double-stranded DNA (dsDNA) with blunt or recessed 3'-end. Single-stranded DNA and dsDNA with 3'-protruding end of 4 or more nucleotides are resistant to cleavage by exonuclease III.¹²⁸ Therefore, to preserve the intactness of the target during the enzyme-catalyzed reaction in an exonuclease III-aided DNA sensor, the signaling probes should have the blunt or recessed 3'-end in the probe-target hybrid (Fig. 16A). A hairpin signaling probe should have the 3'-protruding end, which becomes blunt (or recessed) upon hybridization with the target (Fig. 16B).

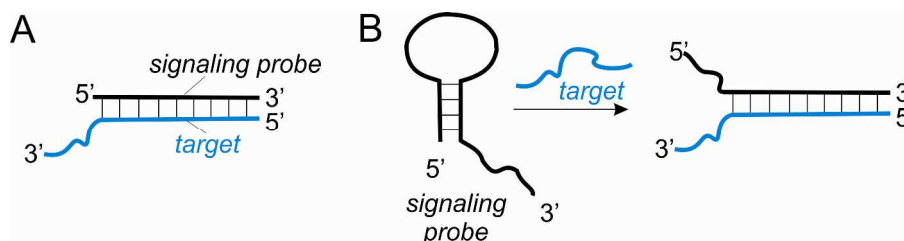


Fig. 16. Structural requirements for a signaling probe in case of exonuclease III-assisted signal amplification assays. (A) In the probe-target complex, the probe should have 3'-blunt end, while the 3'-end of the target should be protruding. (B) In the absence of a target the hairpin probe should possess the 3'-protruding end, which becomes blunt upon hybridization with the target.

An exonuclease III-based approach for signal amplification DNA detection was pioneered by Okano and Kambara.¹²⁹ The authors used a linear probe labeled with a fluorophore at its 5'-end. When hybridized to a target DNA the probe was specifically digested by the enzyme from its 3'-end. Shortening of the probe made the complex between the probe and the target unstable, and the target dissociated to be able to bind to the next available target molecule. The accumulated shortened probes were detected by gel electrophoresis. The authors observed high background signal due to the enzymatic digestion of the free probe. However, this background reaction was caused by the formation of intramolecular double-stranded fragment within the probe, and, therefore, could be controlled by optimizing the sequence of the probe as well as by increasing the assay temperature. The LOD of the assay was ~0.5 pM (0.9 amol in a 2 μL sample). It is interesting to note that the dominant products of the probe digestion were 7-mer oligonucleotides due to dissociation of the short fragments from the target complex at the final stage of digestion. The length of the probe digestion products should be taken into account while designing exonuclease III-assisted assays.

In a number of assays, nanomaterials served for quenching the fluorescence of fluorophore-labeled linear probes.¹³⁰⁻¹³⁶ For this purpose, single walled carbon nanotubes (SWNT),¹³⁰

graphene oxide (GO),¹³¹⁻¹³⁴ carbon nitride nanosheets (CNNS)¹³⁵ and Pd nanowires (NWs)¹³⁶ were employed. These nanomaterials display the affinity to single-stranded DNA, but not to double-stranded DNA, the fluorophore or the fluorophore-containing mononucleotide.⁷⁸⁻⁸² In the absence of the target, the single-stranded probe was bound to the surface, which brought the fluorophore and the quencher in proximity and enabled fluorescence quenching. Hybridization of the target to the probe decreased the affinity of the probe to the nanomaterial. The double-stranded probe-target complex became a substrate for exonuclease III, which degraded the probe releasing either a mononucleotide¹³¹⁻¹³⁶ or a trinucleotide¹³⁰ containing the fluorophore. The affinity of the nanomaterials to the released fluorescent fragments was even lower than that for dsDNA. For the majority of the reported assays, the LOD lied in picomolar or subpicomolar range: 50 pM,¹³⁰ 20 pM,¹³¹ 5 pM¹³² or 0.5 pM.¹³³ Lower LOD obtained by the last group¹³³ can be attributed to the use of a surface blocking agent. Using CNNS as quenchers enabled the LOD of 81 pM, ~26-fold improvement in comparison with “no enzyme” assay.¹³⁵ When Pd NWs were used, the LOD of 0.3 nM was demonstrated, which was shown to be 20-fold lower than in an Exo III-free assay.¹³⁶ Most nanomaterial-based assays are quite fast, with the total assay time within 30-60 min, which is an undoubted advantage of this strategy. Another advantage is the possibility of multiplex nucleic acid detection by using several probes modified with different fluorophores, since the nanomaterials can efficiently quench a variety of fluorophores. This advantage was successfully demonstrated for GO-based^{132,133} and CNNS-based¹³⁵ assays. At the same time, the procedure of nanomaterial preparation is multistep and laborious. In addition, the approach has relatively low selectivity, which is shared with all linear probes. This strategy was employed for the analysis of telomerase activity¹³² and for site-specific determination of DNA methylation¹³⁴ in cancer cells. The telomerase activity could be detected in the extract from at least 250 HeLa cells. Using the luminol-H₂O₂-horse radish peroxidase system as a donor for chemiluminescence resonance energy transfer, as low as 0.002% methylation level could be determined in 0.5 nM mixture of methylated and unmethylated DNA.¹³⁴

The exonuclease III-assisted target recycling was used in combination with a flow cytometry-based DNA bead assay.¹³⁷ In this case, a fluorophore-labeled linear probe was attached to a microsphere. Each cycle of target-mediated degradation of the reporter by the enzyme resulted in the removal of one fluorophore molecule from the microsphere surface, and the decrease in fluorescence intensity of individual microsphere could be detected by flow cytometry. The lowest LOD of 3.2 pM was achieved using high-density probe microspheres. Multiplexing capability of the assay was also demonstrated.

Cui et al. used a displacement probe with exonuclease III-assisted signal amplification strategy.¹³⁸ The displacement probe contained two complementary strands, one of which was labeled with a fluorophore at its 5'-end (fluorophore strand), while another was labeled with a quencher at its 3'-end (quencher strand). The fluorophore strand was shorter than the quencher one to ensure that the probe was not cleaved by exonuclease III in the absence of the target DNA (Fig. 17). The fluorescence of the fluorophore strands was quenched due to the proximity of the quencher group. The target displaced the quencher strand from the duplex forming the fluorophore strand-target complex, in which the fluorescence was restored. Moreover, the complex with the 3'-recessed end was a substrate for exonuclease III. After enzyme-catalyzed degradation of the fluorophore strand, the target could displace another quencher strand from the probe. This strategy allowed detection of as low as 24 pM DNA target within 20 min.

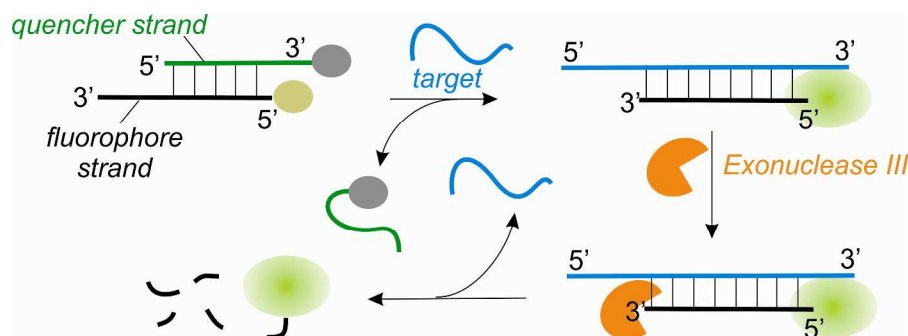


Fig. 17. Displacement probe in an exonuclease III-assisted signal amplification assay.¹³⁸

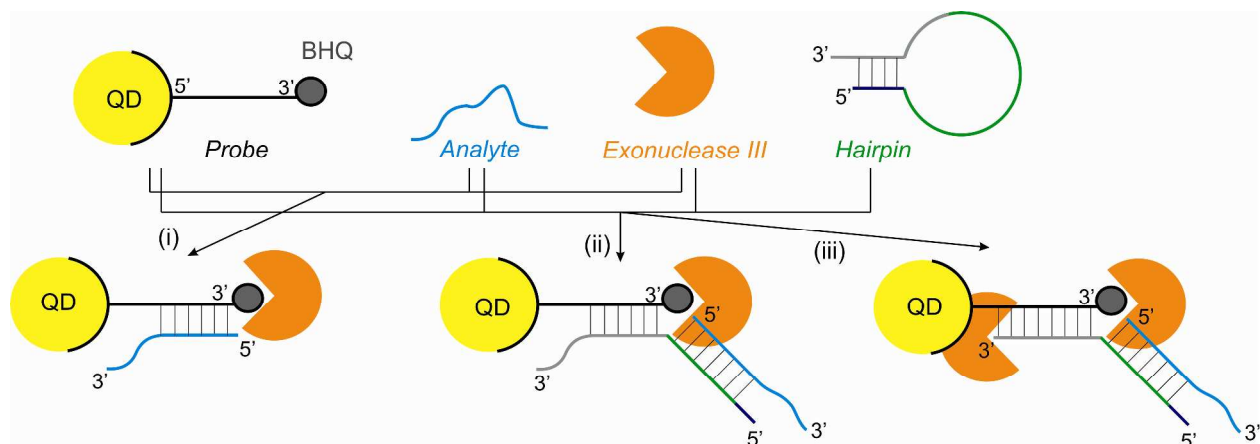


Fig. 18. Three variations of exonuclease III-based signal amplification platform utilizing CdSe/ZnS quantum dots (QD).¹³⁹

Quantum dots as fluorophores were also explored for exonuclease III-based signal amplification.¹³⁹ In one example, a linear probe was labeled with CdSe/ZnS QDs at its 5'-end and with Black Hole quencher (BHQ) at its 3'-end (Fig. 18, i). The LOD for this detection platform was found to be 1 pM. By using QDs of different sizes, the authors demonstrated the implementation of the platform for the multiplexed analysis. In addition, an indirect binding of the QDs-labeled probe to the target was suggested, which overcame the requirement of a specific QD/BHQ-modification for every new target-specific probe. The indirect binding platform utilized a nucleic acid hairpin that contained a loop domain complementary to the target and a conserved sequence, which was caged in the stem portion of the hairpin, complementary to the probe. The conserved sequence of the “adaptor” hairpin was designed either to form 3'-terminal overhang in the complex with the probe (Fig. 18, ii) or to be fully complementary to the probe (Fig. 18, iii). In the case of full complementarity, the exonuclease III digested both the probe and the adaptor hairpin. The indirect sensing assay, however, took longer time than the direct one.

A low LOD of 83 aM for a fluorescently labeled linear probe was demonstrated using fluorescence polarization as a detection technique.¹⁴⁰ The intensity of the signal depended on the freedom of the rotational motion of the fluorophore label. When the probe was intact, the attached fluorophore had limited rotation, and fluorescence anisotropy was high. Exonuclease III-catalyzed cleavage of the probe resulted in liberating the fluorophore-modified mononucleotide, decreasing anisotropy. Enzyme-assisted signal amplification increased the LOD by 6-7 orders of magnitude in comparison with the unamplified assay.

A new type of probes named “linear molecular beacons” (LMBs) was used with exonuclease III-assisted target recycling approach.¹⁴¹ An LMB probe represented a linear single-stranded oligonucleotide, which, like MB probes, had both a fluorophore and a quencher. Both dyes were attached close to the 3'-end of the probe, to the terminal and penultimate nucleotides, respectively (Fig. 19). In the absence of the target, fluorescence of the probe was low due to efficient quenching of the fluorophore by the closely located quencher dye. Hybridization to a specific DNA target resulted in the formation of duplex with a recessed 3'-end at the probe, which was degraded by the enzyme. A fluorophore-modified nucleotide was released in the solution, thus being separated from the quencher, and the fluorescence was restored. The LOD of 120 fM was observed at room temperature. It was lower than the LOD for the displacement probe targeting the same DNA, which resulted from a significant decrease in the background fluorescence of LMB probe. In addition, the LMB probe demonstrated faster hybridization kinetics than the displacement probe. Even lower LOD of 25 fM was observed when nonspecific background enzyme-mediated cleavage of LMB probe was suppressed by reducing the temperature to 4°C.

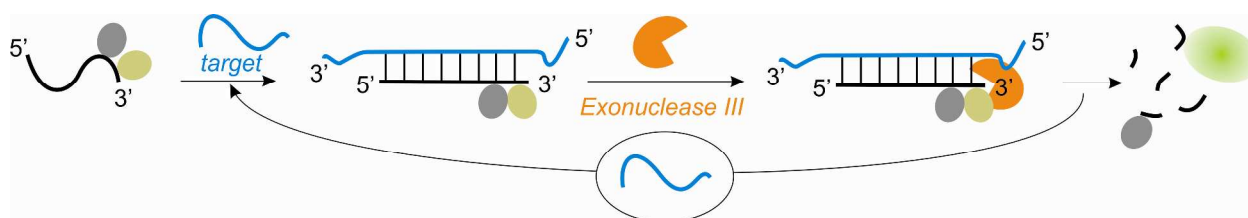


Fig. 19. Exonuclease III-assisted signal amplification assay with a “linear molecular beacon” probe.¹⁴¹

The exonuclease III-based signal amplification strategy was also employed for hairpin hybridization probes. Assays with fluorescent readout used MB probes as reporters.^{142,143} To minimize the background digestion of the probe in the absence of the target, it was designed to have the 3'-protruding end (Fig. 20). Black Hole quencher was attached to an internal position close to the 3'-end of the probe. In the close conformation of the MB probe the quencher was situated in the proximity to the fluorophore enabling efficient fluorescence quenching. In the probe-target complex, the quencher was separated from the fluorophore, and the fluorescence was partially restored. Enzymatic cleavage of the probe in the complex substantially increased fluorescence due to the release of the fluorophore-containing short oligonucleotide in solution. The detection limit of 10 pM was achieved after 30 min at 37 °C, which was considerably lower than without amplification of the signal (7.8 nM).¹⁴² Under these conditions the enzyme-aided target recycling led only to a 4-fold signal increase over the background due to the background cleavage of the free probe by exonuclease III. In order to abolish the background reaction, the assay was performed at 4 °C, resulting in the LOD of 20 aM.¹⁴² Unfortunately, these new conditions required 24 h to complete the assay. This value is among the lowest detection limits for PCR-free assays reported so far, which is an undoubted advantage of the suggested strategy. Alternatively, digestion-resistant locked nucleic acids (LNA) were introduced in the stem of the MB probe.¹⁴³ This modification enabled rapid detection of 30 fM synthetic DNA target at 37 °C. The LNA-MB probe-based strategy was employed by the authors for monitoring of telomerase activity.¹⁴³ For this purpose, the probe targeted the telomeric repeat sequence, which was synthesized by telomerase by elongating a primer. As few as 30 breast cancer cells were shown to be enough to detect telomerase activity.

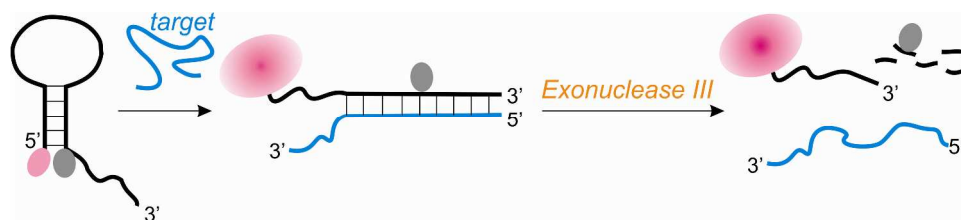


Fig. 20. Exonuclease III-assisted signal amplification with molecular beacon probes.^{142,143}

To enable fluorescent readout, labeling of the signaling probes with a fluorescent tag is required, which adds to the cost of the assay. Several label-free fluorescent or chemiluminescent assays were reported.¹⁴⁴⁻¹⁴⁸ A simple assay utilized a label-free hairpin probe and a nucleic acid dye SYBR Green I.¹⁴⁴ The dye strongly binds to the double-stranded DNA. In the absence of a target DNA the probe had a stem region attracting the dye, and the fluorescence was high. Hybridization of the probe to the target and its enzymatic cleavage removed double-stranded regions suitable for SYBR Green I binding. The signal decreased. This simple assay demonstrated the LOD of 160 pM for a synthetic DNA target. The linear range was from 0.3 to 2.5 nM. Another approach took advantage of G-quadruplex complexes with porphyrins or thioflavin.¹⁴⁵⁻¹⁴⁷ In two reports, a duplex DNA probe was employed.¹⁰⁷ The probe contained two 3'-terminal single-stranded fragments, which secured the probe from degradation by exonuclease III in the absence of the target (Fig. 21A). One strand of the probe contained a target-recognition domain on its 3'-end, while another strand was a G-quadruplex-forming oligomer and served as a signal reporter. In the presence of a specific DNA target, the probe strand with the blunt 3'-end in the probe-target complex was degraded by exonuclease III, and the signal reporter was liberated. The active G-quadruplex bound *N*-methyl mesoporphyrin¹⁴⁵ or Thioflavin T¹⁴⁶ and consequently enhanced their fluorescence. The LODs for the assays were found to be 36 pM¹⁴⁵ and 20 fM.¹⁴⁶ Improved detection limit in the later report was attributed to the optimized sequence of the G-rich probe, as well as to lower background provided by higher structural selectivity of the thioflavin for G-quadruplexes.¹⁴⁶ The ability of G-quadruplex to increase the fluorescence of *N*-methyl mesoporphyrin was also used in combination with RCA, with LOD of 2.5 pM.¹⁴⁷

The label-free chemilumnescent assay made use of a peroxidase-like activity of a hemin-G-quadruplex complex using luminol as an oxidizable substrate.¹⁴⁸ The G-quadruplex-forming sequence was a part of a hairpin probe (Fig. 21B). In the presence of a DNA target, exonuclease III digested the portion of the hairpin probe complementary to the target, thus releasing the active G-quadruplex-forming sequence in solution and generating the signal. High background resulted from luminol oxidation by the unbound hemin was decreased by capturing the excess of free hemin by SWNTs. The use of SWNTs enabled improvement of the LOD about 10-fold, from 0.1 pM to 12 fM.

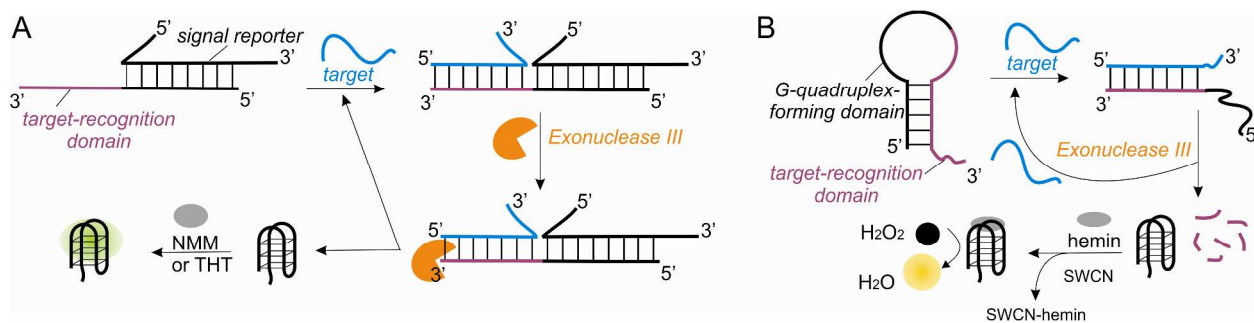


Fig. 21. Label-free fluorescent or chemiluminescent assays based on G-quadruplex formation. (A) Duplex probe contained a G-quadruplex-forming reported strand, which folded into the active structure after degradation of the second strand of the probe, allowing high fluorescent signal produced by G-quadruplex-bound *N*-methyl mesoporphyrin IX (NMM)¹⁴⁵ or Thioflavin T (THT).¹⁴⁶ (B) Chemiluminescent assay with decreased background due to absorption of hemin by SWNT.¹⁴⁸

The research group of Yang developed a universal platform to detect DNA with colorimetric/visual signal output.¹⁴⁹ The platform made use of two types of oligonucleotide-modified gold nanoparticles and an oligonucleotide strand serving as a linker between them. In addition to being complementary to the oligonucleotides attached to gold nanoparticles, the linker was designed to hybridize to target DNA. In the absence of the target, the linker strand brought two gold nanoparticles into proximity by hybridizing to the oligonucleotide strands attached to them. The color of solution turned purple. In the presence of the target DNA, the linker-target duplex with a recessed 3'-end was processed by exonuclease III, which cleaved the linker strand. At the final stage, little or no linker strands were available to connect gold nanoparticles to each other, and the color remained red. The detection limit of 15 pM was achieved.

Another approach for label-free colorimetric/visual DNA detection was suggested by Bi and colleagues.¹⁵⁰ In this approach called “exonuclease-assisted cascaded recycling amplification” (Exo-CRA), a target DNA triggered the assembling of a DNA nanoball with branched DNA structures from three types of unlabeled hairpin oligonucleotides (Fig. 22). One of the hairpin oligonucleotides (MB1) served as both the reactant and signaling probe. It had a target-recognition domain at the 3'-end and the G-quadruplex-forming sequence at the 5'-end. Two other hairpin oligonucleotides (MB2 and MB3) acted as transducers to drive the cascading. In the absence of the target DNA, the oligonucleotides self-hybridized in stable stem-loop structures containing 3'-protruding ends that prevented their background cleavage by exonuclease III. The G-quadruplex-forming sequence was “caged” in the stem region of MB1 and thereby inactive. The target triggered the DNA nanoball formation by opening up MB1, which, in turn, hybridized to a fragment of MB2 making it available for binding to MB3. As a result, several double-stranded fragments with blunt 3'-ends were formed, which could be recognized as substrates for exonuclease III. After enzyme-mediated cleavage, three types of short oligonucleotide strands were released: one serving as a trigger for the next hybridization/cleavage event; one serving both as a trigger and as a signal reporter; and one containing the target sequence (target recycling). The signal reporter folded in the G-quadruplex structure, which bound hemin and catalyzed oxidation reaction leading to the color change (Fig. 22). The strategy allowed detection of as low as 0.1 pM DNA with the dynamic range of 8 orders of magnitude. The use of three hairpin probes instead of just one enabled 100-fold improvement in the LOD. Along with visual signal and low detection limit, an advantage of this strategy is that only one hairpin, MB1 containing target-recognition domain, needed to be changed for any new target DNA sequence. Starting with a single-stranded DNA target, the total assay time was about 30 min.

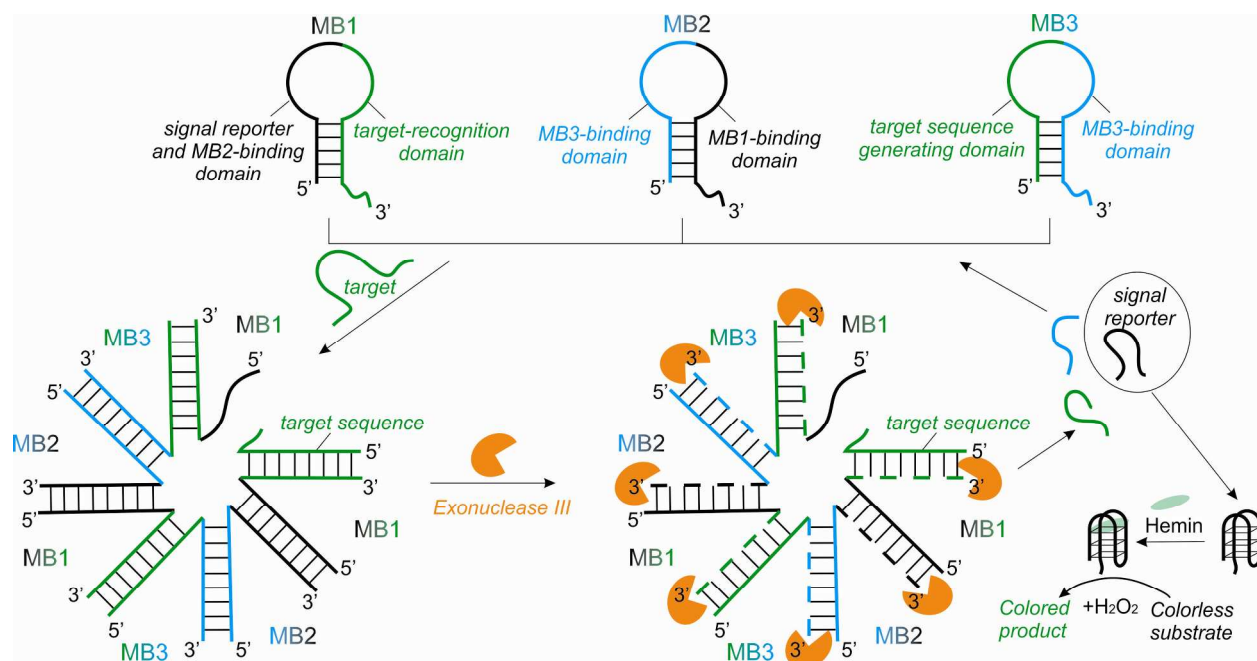


Fig. 22. Colorimetric detection of DNA based on exonuclease-assisted cascaded recycling amplification using label-free hairpin probes.¹⁵⁰

Similar strategy for label-free visual detection of HIV DNA utilized two instead of three unmodified hairpin probes for signal amplification.¹⁵¹ Both probes contained the G-quadruplex sequence in their 5'-terminal fragments. One of the probes also contained a target-recognition domain, while another – a sequence complementary to the loop portion of the first hairpin. Two semi-independent cycles of exonuclease III-catalyzed cleavage of the probes generated active G-quadruplex sequences. The G-quadruplex-hemin complex then catalyzed ABTS oxidation generating a visual signal. As low as 2.5 pM target could be detected with the possibility to discriminate single-base mismatched targets from the perfectly matched DNA.

Several groups have reported electrochemical DNA sensors that utilize exonuclease III-assisted signal amplification.¹⁵²⁻¹⁶² Both heterogeneous and homogeneous electrochemical assay formats were used. In case of heterogeneous assays, a DNA probe was immobilized on the electrode surface, and the enzymatic cleavage of the probe occurred on the surface of the electrode. In homogeneous format, the probe-target hybridization and enzyme-catalyzed degradation of the probe took place in solution. Homogeneous electrochemical detection has an advantage of faster DNA hybridization and enzyme catalysis, as well as simpler procedure for preparation of an electrode. For both assay formats, an electro-active “tag” can be covalently attached to the probe. Alternatively, a label-free design is possible, where redox tag is bound to the probe and/or probe-target complex by non-covalent interactions (electrostatic interaction, intercalation, etc.). In this case, the difference in electrochemical signal is achieved due to the difference in the rate of diffusion between free and probe-bound redox tag.

A label-free heterogeneous assay for signal-OFF electrochemical DNA detection was developed with a linear unlabeled probe immobilized on the gold electrode.¹⁵² In the absence of target DNA, electrostatic interaction of the probe with a redox mediator $[\text{Ru}(\text{NH}_3)_6]^{2+/3+}$ allowed electron transfer between the mediator and the electrode producing high redox signal (Fig. 23, left). Exonuclease III selectively cleaved the target-bound probe into mononucleotides. After

several probe cleavage cycles, the majority of the electrode-immobilized probe molecules were degraded, and the redox mediator could no longer bind close to the electrode surface. The redox signal was low (Fig. 23, right). At the optimized surface probe density, the sensor demonstrated the LOD of 20 fM. The selectivity of DNA detection increased with the number of mismatches in the probe-target hybrid, and the signal triggered by 4-nt mismatched DNA was close to the background. The total assay time was 2 hrs at room temperature.

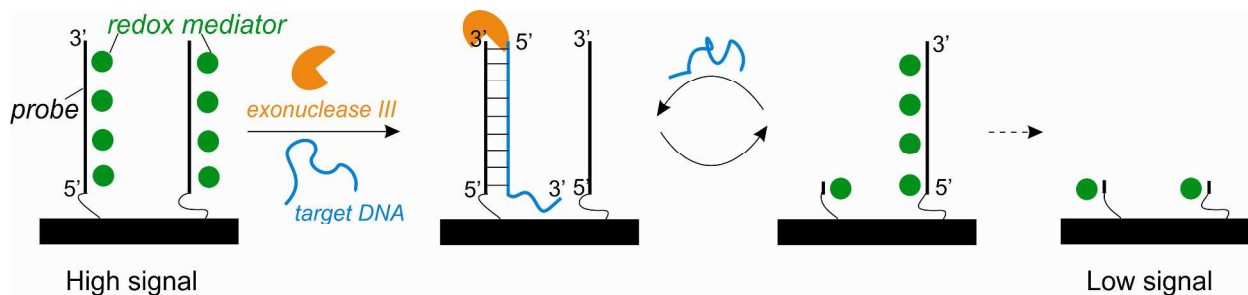


Fig. 23. A label-free strategy for signal-OFF electrochemical detection of DNA with a linear probe.¹⁵² A redox mediator $[\text{Ru}(\text{NH}_3)_6]^{2+/3+}$ is bound to the probe by electrostatic interactions.

Another signal-OFF electrochemical biosensor utilized a linear capture probe attached to a gold electrode and a linear biotinylated detection probe in solution (Fig. 24).¹⁵³ In the absence of a nucleic acid target, the capture probe hybridized with the detection probe followed by incubation with streptavidine-alkaline phosphatase conjugate (St-AP) and a substrate for alkaline phosphatase, such as α -naphthyl phosphate. The enzymatic hydrolysis on the electrode surface produced electrochemical signal (Fig. 24A). The target DNA bound to the capture probe forming a duplex, in which the probe was degraded by exonuclease III. As a result, the amount of the capture probe on the electrode surface available for hybridization with the detection probe decreased, and the signal decreased accordingly (Fig. 24B). The detection limit of 8.7 fM was achieved with a linear range 0.01 pM – 1 nM. The assay allowed selective detection of *Escherichia coli* in milk samples down to 40 CFU/mL. Other bacteria – *Streptococcus pneumoniae*, *Pseudomonas aeruginosa*, α -hemolytic *streptococcus* – triggered the signal close to background, proving good selectivity of the approach. The assay requires incubation of the electrode at 37 °C with the target and the enzyme for 2 h, then with the detection probe for 1 h, with St-AP for 30 min, and, finally, with α -naphthyl phosphate prior to detection.

A homogeneous label-free assay with electrochemical readout was developed.¹⁵⁴ The assay used a displacement probe, which consisted of two complementary non-labeled oligonucleotide strands forming a duplex with 3'-protruding ends (similar to that depicted in Fig. 17). An osmium complex that tends to intercalate into dsDNA was used as a redox indicator. In the absence of the target, the redox indicator was bound to the probe, and the signal was low due to the lower diffusion rate of the bound indicator to the electrode. The target displaced one of the strands from the double-stranded probe forming another dsDNA structure with one of the 3'-ends (at the probe strand) being blunt or recessed. Exonuclease III catalyzed degradation of the target-bound fragment of the probe, thus decreasing the amount of the intact double-stranded probe or probe-target complex available for the redox indicator to bind. The detection limit for the assay was found to be 2.5 nM after 10 min of incubation with the enzyme.

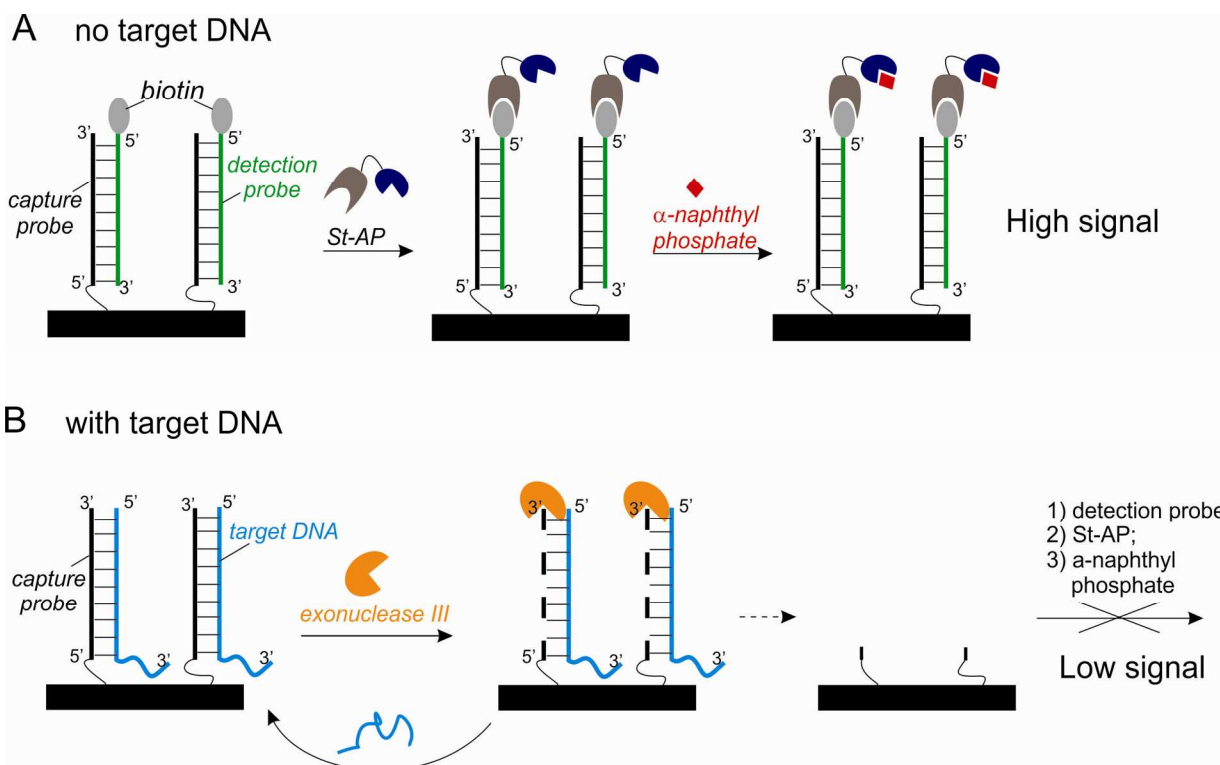


Fig. 24. Electrochemical signal-OFF biosensor used for the detection of enteropathogenic bacteria.¹⁵³ (A) In the absence of the target DNA, a biotinylated detection probe bound to the electrode surface via hybridization to an immobilized capture probe. The duplex was recognized by streptavidine-alkaline phosphatase (St-AP), which bound α -naphthyl phosphate, thus permitting electrochemical signal. (B) When target was present, it hybridized to the capture probe, which was cleaved by exonuclease III. After several rounds of hybridization/cleavage, the majority of the capture probe was degraded, and the detection probe could not approach to the electrode surface; the signal decreased.

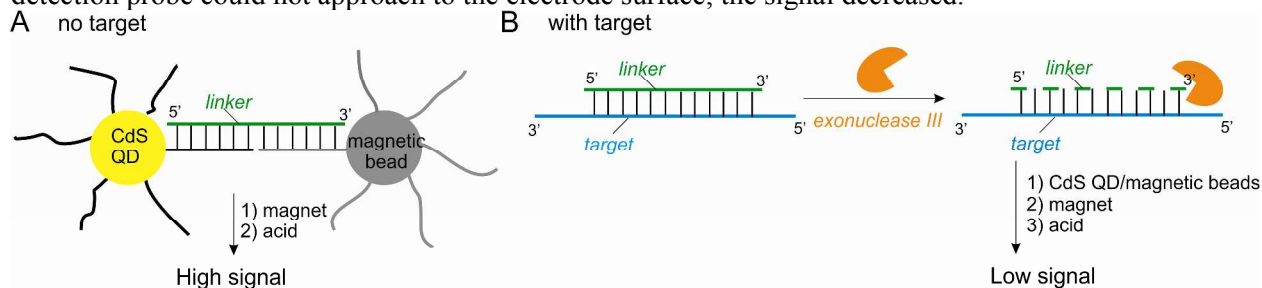


Fig. 25. Dual signal amplification strategy.¹⁵⁵ (A) In the absence of the target a linker oligonucleotide connected CdS quantum dots (QD) with magnetic beads by hybridizing to QD- and beads-attached oligonucleotide strands. After magnetic separation of the complex from free CdS QD and acid dissolution of separated CdS QD, the released Cd^{2+} ions were detected by square wave voltammetry, and the signal was high. (B) The linker hybridized to the target DNA forming the recessed 3'-end; exonuclease III recognized the linker-target hybrid and degraded the linker, which could no longer connect QD with magnetic beads. The separated magnetic beads did not contain CdS, and upon acid treatment the signal was low.

A dual signal amplification strategy combining exonuclease III-assisted target recycling with the CdS QD layer-by-layer (LBL) assembly amplification was described by Su and co-

authors.¹⁵⁵ Electrochemical signal of the system relied on the detection of Cd^{2+} ions, which were released from QDs upon acid treatment. To capture the signal-producing QDs, magnetic beads were used. Both QDs and magnetic beads were functionalized with short oligonucleotides, which were complementary to the fragments of a linker strand (Fig. 25A). In the absence of a target DNA, the linker connected QDs to the beads enabling magnetic separation of free QDs from those bound to the linker. Acid treatment of the captured QDs generated high electrochemical signal. When target was present, it hybridized to the linker and triggered its degradation by exonuclease III (Fig. 25B). The degraded linker could no longer connect CdS QDs to the magnetic beads. As a result, no Cd^{2+} was present to produce electrochemical signal after magnetic separation. The signal decreased with the decreased amount of intact linker in solution, which, in turn, depended on the concentration of the target DNA. With that system, the authors targeted a fragment of the 16S rRNA gene (nt 432-461) from the *Escherichia coli* uropathogenes and achieved the LOD of 5 fM.

A heterogeneous signal-OFF electrochemical assay was developed with a hairpin probe immobilized on a graphene/Au nanocomposites-modified carbon electrode.¹⁵⁶ In its stem-loop conformation, the probe had a 7-nt protruding 3'-end, which protected the free probe from exonuclease III-catalyzed degradation. A specific DNA target hybridized to the probe making its 3'-end recognizable by the enzyme. The signal depended on redox conversion of the electrochemical indicator $[\text{Fe}(\text{CN})_6]^{3-/4-}$ on the electrode. In the absence of the target, as well as in the presence of the target but without exonuclease III, the negatively charged DNA repelled the indicator from the electrode, which resulted in high electrode transfer resistance. Degradation of the electrode-immobilized probe resulted in decreased resistance. The assay provided the detection limit of 10 fM and a dynamic range of 50 fM - 5 nM.

Fan and colleagues used gold nanoparticles for dual signal amplification to detect a synthetic target related to human immunodeficiency virus (HIV).¹⁵⁷ Gold nanoparticles were functionalized with a short oligonucleotide served as a reporter. The reporter was complementary to the 5'-terminal fragment of an electrode-immobilized hairpin probe. In the absence of a target, this fragment was blocked from interaction with the reporter in the stem, and the hairpin probe was resistant to cleavage by exonuclease III due to its 3'-protruding end. The presence of a target DNA opened up the hairpin probe on the electrode surface and triggered its cleavage by the enzyme. Since the target was not complementary to the 5'-terminal fragment of the probe, the enzyme left this electrode-immobilized fragment intact. It then hybridized to the reporter, thereby loading the gold nanoparticles onto the electrode. The formed structure could bind multiple $[\text{Ru}(\text{NH}_3)_6]^{3+}$ electroactive labels via electrostatic interactions, enabling electrochemical response. The LOD was found to be 33 pM.

Another signal-ON electrochemical biosensor utilizing gold nanoparticles took advantage of dual signal amplification strategy.¹⁵⁸ The strategy combined exonuclease III-assisted target recycling with a nanoparticle-based super-sandwich approach to amplify the signal. The assay consisted of two steps. Interaction of a hairpin probe with the specific target and enzymatic cleavage of the target-bound probe took place in solution (Fig. 26A). Since the target was complementary only to the 3'-fragment of the probe, a short 5'-terminal probe fragment was released after cleavage. It interacted with another hairpin probe – a capture probe immobilized on a gold electrode (Fig. 26B). After hybridization, the capture probe contained a “sticky end”, which was complementary to an oligonucleotide attached to a gold nanoparticle. Interaction of the electrode-immobilized complex with the oligonucleotide-functionalized nanoparticles produced a super-sandwich-like structure. The structure captured multiple molecules of an

electrochemical indicator methylene blue, which increased the signal on the electrode. Employment of the dual amplification strategy resulted in about 4-fold signal increase in comparison with either target recycling or nanoparticle-based super-sandwich strategy alone. The LOD of 0.6 pM for a synthetic DNA target was demonstrated. High selectivity of the hairpin probe enabled differentiation between SNP-containing targets. In addition, the assay is easily adapted for any new target, since the sequence of only one label-free hairpin probe needs to be changed.

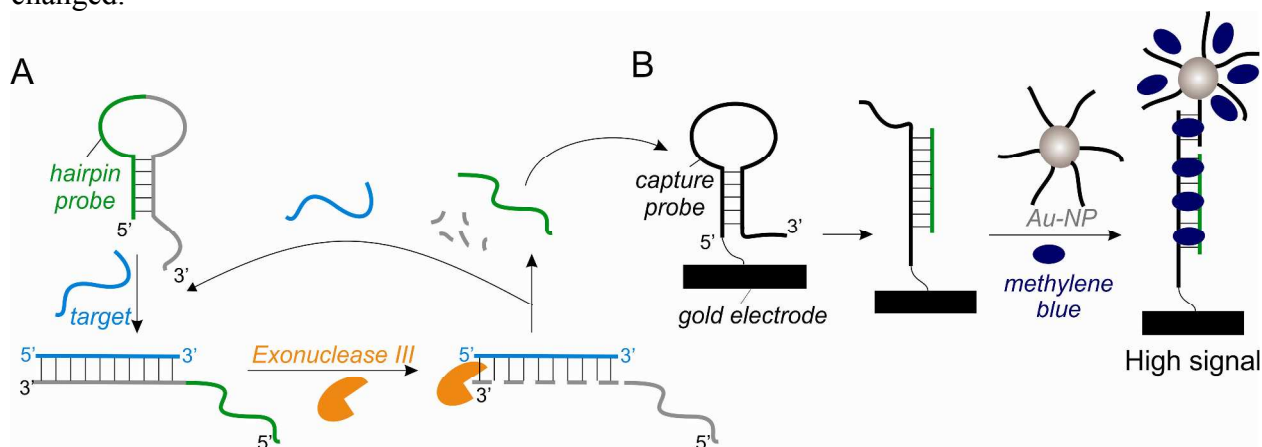


Fig. 26. Electrochemical signal-ON biosensor based on a dual signal amplification strategy with super-sandwich-like detection.¹⁵⁸ (A) Homogeneous target-recycling step. (B) Heterogeneous electrochemical detection step.

An elegant approach for homogeneous signal-ON electrochemical assay was pioneered by a Hsing and co-authors.¹⁵⁹ In their design, an electrochemical molecular beacon (eMB) probe with a 7-nt 3'-protruding end containing methylene blue label was used as a signal reporter. This probe was not attached to the electrode, and the target detection was achieved due to the difference in diffusivity between an oligonucleotide and a mononucleotide toward a negatively charged indium tin oxide (ITO) electrode. In the absence of the target, eMB demonstrated negligible electrochemical response due to electrostatic repulsion from the electrode. When the target DNA was present, it hybridized to the eMB probe to form 3'-blunt end, which was recognized by exonuclease III. The enzyme degraded the eMB probe releasing an electro-active methylene-blue labeled mononucleotide, which diffused to the ITO electrode and caused an increase of the electrochemical signal. The detection limit for the probe was found to be 20 pM after 1 h. At the same time, the developed endonuclease III-assisted MB-based electrochemical sensor demonstrated poor selectivity: a target with a single-nucleotide mismatch triggered the signal 71 % of that of the perfectly matched DNA target. Recently, another research group modified the immobilization-free eMB approach to improve the LOD down to 0.1 pM by employing two autonomous cyclic production of the free electro-active mononucleotide.¹⁶⁰ In the modified design, the target-recognition domain of the ferrocene-labeled hairpin probe was limited to the 3'-protruding fragment of the probe. The target-triggered digestion of the probe by exonuclease III in the first cycle generated a secondary target analog that could trigger another cycle of the probe degradation and be recycled along with the target to further amplify the signal.

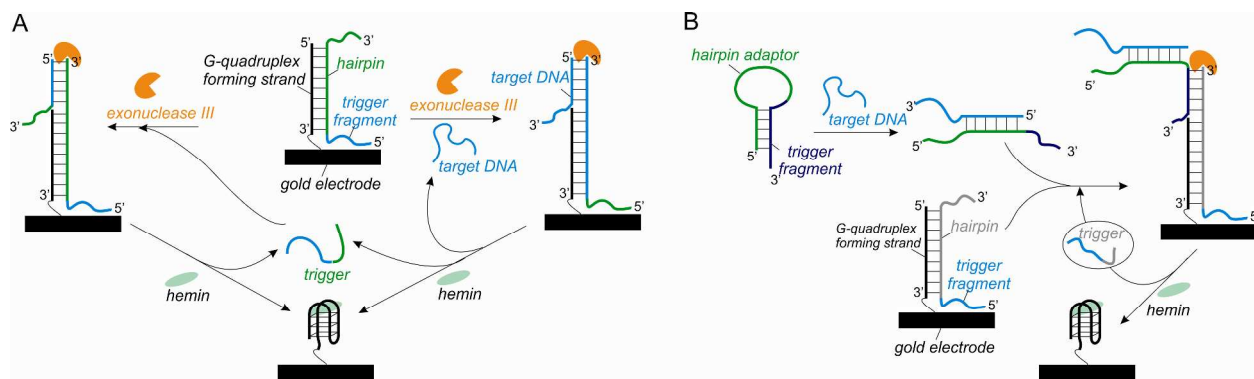


Fig. 27. Electrochemical DNA detection using exonuclease III-assisted autocatalytic target recycling strategy.¹⁶¹ (A) Two cycles enabled exponential signal amplification. (B) Modification of the assay utilizes an additional hairpin adaptor oligonucleotide to enable sensing of any DNA sequence. Instead of hybridizing to the double-stranded probe directly, the target binds to the hairpin adaptor, thus opening it up and allowing its hybridization to the probe. The probe-target hybrid then undergoes cleavage by the enzyme leading to the high signal.

Duplex DNA probes self-assembled on the surface of a gold electrode were also used to design electrochemical DNA sensors.^{161,162} In one strategy, the duplex probe was formed by hybridization between a hairpin strand and a 3'-thiol modified linear strand covalently attached to the electrode's surface (Fig. 27A).¹⁶¹ The linear strand contained a G-quadruplex-forming structure, which was inactivated by hybridization with the hairpin strand of the probe. The hairpin probe contained a target-recognition domain in its stem region. Upon addition of the target, the double-stranded probe-target complex was formed, in which the 3'-end at the hairpin strand became blunt. Consequently, exonuclease recognized the complex and degraded the hairpin strand liberating the G-quadruplex-forming strand. The G-quadruplex bound hemin on the electrode surface. The electrochemical reduction of the bound hemin produces a signal detected by differential pulse voltammetry. The enzyme-catalyzed degradation of the hairpin strand also released the target and a fragment of the hairpin strand (trigger fragment) that was complementary to the intact hairpin strand and could start the target recycling, thus further amplifying the signal (Fig. 27A). Therefore, instead of one amplification cycle of reactions, the assay contained two cycles, which allowed exponential signal amplification. The LOD for the assay was 10 fM, which provided 100-fold improvement over conventional (single-cycling) signal amplification strategy. The assay was also highly selective allowing discrimination of the targets differing in a single nucleotide. In addition, the authors developed a versatile design of the assay, which used the same probe for the detection of any target. It was achieved with the help of an additional hairpin strand containing the target-recognizing domain in the loop and the probe-binding domain in the stem (Fig. 28B). Another strategy was based on the specific affinity of methylene blue used as a redox indicator to the unbound guanine bases.¹⁶² For this purpose, the covalently attached strand of the probe was made guanine-free, while the longer strand contained 5'-terminal G-rich single-stranded fragment. In the absence of the target the electrochemical signal was high due to specific binding of the indicator to the G-rich fragment of the probe. In the presence of the target, the longer strand of the probe became digested by exonuclease III, and the G-rich fragment was removed from the electrode's surface, which decreased the amount of the indicator bound to the electrode. The approach demonstrated the LOD of 20 fM for a synthetic DNA target.

Exonuclease III-aided signal amplification strategy was also used in a format of DNA microarrays.¹⁶³ In this work an array of linear probes was created on gold-modified slides by attaching them to the surface via their 5'-ends. In the presence of a DNA target, a probe-target duplex with the blunt or recessed 3'-terminus at the probe was formed and digested by exonuclease III. The signal was detected with surface plasmon resonance (SPR) imaging. The authors reported that upon recognition of the double-stranded probe-target substrate, exonuclease III was able to completely remove the single-stranded DNA probe from the surface, and the background cleavage of the probe in the absence of the target was not observed. The limit of detection for the assay in the range of 10-100 pM was two orders of magnitude better than that without exonuclease-assisted signal amplification.

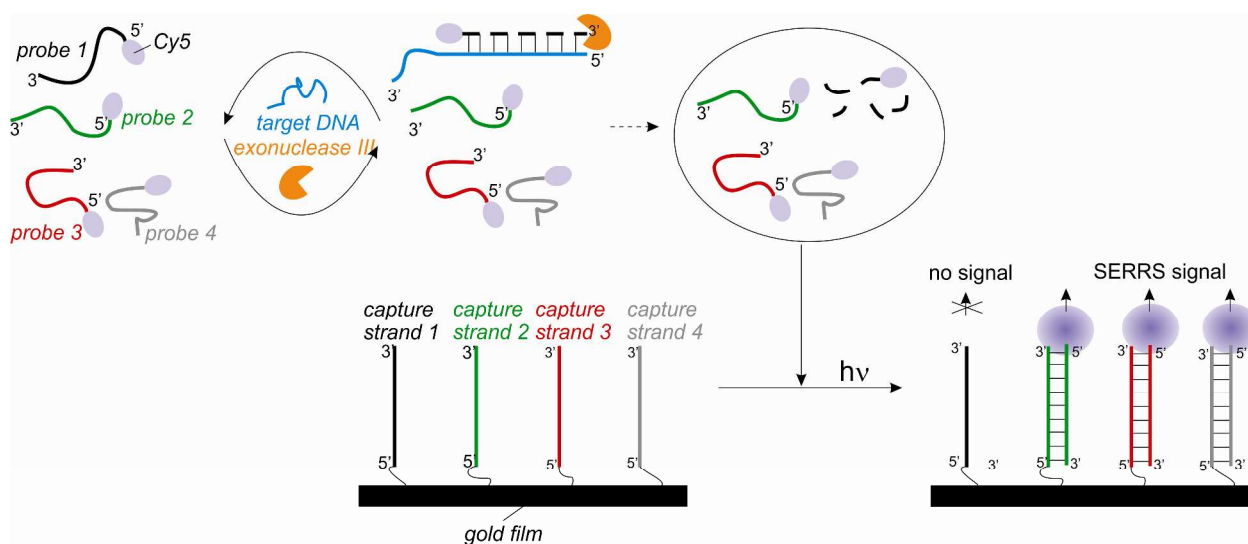


Fig. 28. Multiplex detection of pathogenic fungal DNAs with a nanowire SERRS sensor together with exonuclease III-aided target recycling.¹⁶⁴

Combination of exonuclease III-assisted target recycling with a patterned gold nanowire (Au NW)-on-film surface-enhanced resonance Raman scattering (SERRS) allowed detection of 100 fM DNA targets (3 amole in a 30 μ L sample).¹⁶⁴ A capture DNA strand was attached to an Au NW. The capture DNA was complementary to a specific Cy5-labeled DNA probe, which, in turn, recognized its specific target DNA. Four Au NWs containing four different capture DNA strands were prepared to enable multiplex detection of DNAs from pathogenic fungi causing infections in immunocompromised patients (Fig. 28). When the four probes were mixed with a target DNA, it hybridized to the specific probe forming the duplex with the blunt 3'-end at the probe. After exonuclease III treatment, only the non-specific probes remained intact. They hybridized to the complementary capture DNA strands on the surface of the patterned NW-on-film SERRS sensor, so Raman signal from Cy5 could be detected upon excitation. The NW position containing capture strand complementary to the digested probe showed no SERRS signal, thus revealing the nature of the DNA target. The LOD of 100 fM was reported. The NW SERRS sensor performed equally well with synthetic targets, DNAs extracted from pathogens, and real clinical samples.

Table 3 contains a summary of the described exonuclease III-dependent assays with the focus on the LOD. For the majority of fluorescent assays, the LOD was in picomolar or subpicomolar range. Unusually low LOD of 2.5 pM for an assay with a visual readout was reported for a “nanoball” strategy. The lowest LOD values were reported for the assays with either

electrochemical or fluorescent anisotropy readout. Combination of target recycling with an additional amplification strategy, for example, super-sandwich or QD LBL assemblies, helped to improve the LOD.

Table 3. The LOD for the reported exonuclease III-assisted target recycling assays.^a

Signal readout	Probe	LOD	Ref.
Fluorescence with gel electrophoresis	LP	~0.5 pM (0.9 amol in a 2- μ L sample), with S/B of 2 using M13 mp18 phage DNA	129
Fluorescence	LP/SWNT	50 pM	130
	LP/GO	20 pM	131
		5 pM	132
		0.5 pM	133
	LP/ CNNS	81 pM	135
	LP/ Pd NWs	0.3 nM	136
	LP/magnetic beads/RCA/G-quadruplex	2.5 pM	147
	Displacement probe	24 pM	138
	DLP/QDs	1 pM	139
	LMB	120 fM (room temperature); 25 fM (4 $^{\circ}$ C)	141
	MB	10 pM (37 $^{\circ}$ C); 20 aM (4 $^{\circ}$ C)	142
	MB with LNA	30 fM	143
	HP/SYBR Green I	160 pM	144
	Duplex probe/ G-quadruplex/NMM	36 pM	145
Duplex probe/ G-quadruplex/Thioflavin T	20 fM	146	
Fluorescence with flow cytometry	LP/microspheres	3.2 pM	129
Fluorescent anisotropy	LP	83 aM	140
Chemiluminescence	HP/G-quadruplex/ hemin/luminol	0.1 pM; 12 fM (with SWNT)	148
Colorimetric/visual	Three HPs/ G-quadruplex/hemin/ABTS	0.1 pM	150
	Two HPs/ G-quadruplex/hemin/ABTS	2.5 pM	151
Electrochemical	Label-free LP/[Ru(NH ₃) ₆] ^{2+/3+}	20 fM	152
	LP/biotin/St-AP	8.7 fM; 40 CFU/mL of <i>E. coli</i> in milk	153
	Label-free displacement probe / Os[(bpy) ₂ (dppz)] ²⁺	2.5 nM	154

	LP/QDs/magnetic beads	5 fM	155
	Label-free HP/[Fe(CN) ₆] ^{3-/4-}	10 fM	156
	Label-free HP/ Au-NP/[Ru(NH ₃) ₆] ^{2+/3+}	33 pM	157
	Two label-free HPs/ Au-NP/methylene blue	0.6 pM	158
	eMB	20 pM	159
		0.1 pM	160
	Duplex probe/ G-quadruplex/hemin	10 fM	161
	Duplex probe/methylene blue	20 fM	162
Surface plasmon resonance	LP	10-100 pM	163
Surface-enhanced resonance Raman scattering	LP	100 fM of a synthetic 36-nt DNA and a 307-bp fragment from <i>Aspergillus fumigatus</i> DNA	164

^aSome probe types are abbreviated as for Table 1. SWNT – single walled carbon nanotubes; GO – graphene oxide; NWs – nanowires; CNNS – carbon nitride nanosheets; Au-NP – gold nanoparticles; LMB – linear molecular beacon probe; LNA – locked nucleic acids; NMM – *N*-methyl mesoporphyrin; St-AP – streptavidin-alkaline phosphatase conjugate; eMB – electrochemical molecular beacon (HP labeled with methylene blue or ferrocene); S/B – signal-to-background ratio.

4.2. Lambda exonuclease-assisted assays

Exonuclease from bacteriophage λ rapidly and processively degrades DNA in the 5'→3' direction producing 5'-mononucleotides. The preferable substrate for the exonuclease is double-stranded DNA with 5'-terminal phosphate. The enzyme is capable of digesting non-phosphorylated double-stranded and single-stranded DNA, but at a greatly reduced rate.^{165,166} Therefore, the single-stranded DNA probe usually contains a terminal 5'-phosphate group. Upon hybridization with the target, the probe strand is degraded by the enzyme, and the intact DNA target is “recycled” (as shown in Fig. 1A). *The enzyme cannot process RNA-DNA hybrid; thus the application is limited to the detection of DNA analytes.*

Electrochemical assays based on λ exonuclease-assisted target recycling used either a labeled hairpin probe¹⁶⁷ or a label-free linear probe.¹⁶⁸ The probes were immobilized on the electrode surface via their 3'-ends, while their 5'-ends were phosphorylated. The hairpin probe contained an internal methylene blue label in the loop portion (Fig. 29A). In the absence of the target the electro-active label was away from the electrode, producing a small faradaic current (Fig. 29A, left). The target hybridized to a fragment of the hairpin probe between its 5'-end and the inserted label (Fig. 29A, middle). Hence, λ exonuclease degraded only the target-bound portion of the probe and halted when it reached the single-stranded methylene blue-containing fragment. Therefore, the rigid stem-loop structure of the probe was permanently transformed into a flexible linear structure with the electro-active label close to the electrode's surface thus generating an increased faradaic current (Fig. 29A, right). Unfortunately, the reported electrochemical DNA sensor suffered from low specificity. Even a non-cognate target triggered a signal that was 26% from that of the perfectly matched target. Only the targets containing five or more mismatches

could be discriminated. The LOD for the exonuclease-assisted sensor was found to be about 2 nM, while the sensor without signal amplification detected as low as 10 nM target. High LOD and low efficiency of the signal amplification can be attributed to the exhaustion of the available probe on the electrode's surface, as well as limited selectivity of λ exonuclease for double-stranded DNA, which generated high background signal by digesting the hairpin probe. This problem seems to be absent in case of linear probes. For the label-free linear probe, a model target corresponding the BRCA1 breast cancer gene could be detected with the LOD of 42 pM.¹⁶⁸ In this approach, the electrochemical signal relied on the attraction of a redox indicator $[\text{Fe}(\text{CN})_6]^{3-/4-}$ to the electrode surface. In the absence of the target, the negatively charged indicator was repelled from the electrode due to a compact negatively charged layer formed by the phosphate backbone of the immobilized probe (Fig. 29B, left). In the presence of the target, the probe was digested by the enzyme, allowing the indicator to approach the electrode and generate high signal (Fig. 29B, right).

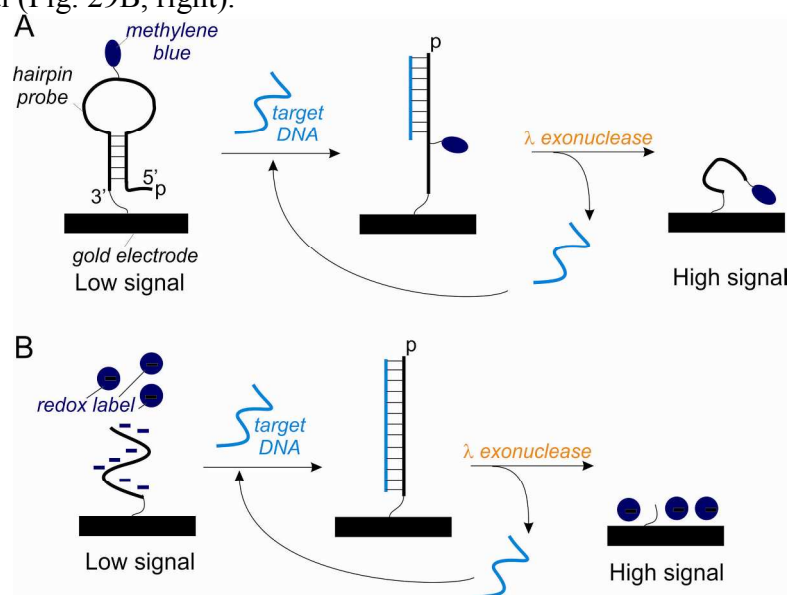


Fig. 29. Electrochemical sensors for nucleic acids based on λ exonuclease-assisted signal amplification. (A) A hairpin probe equipped with a redox label is digested by the enzyme in the presence of the target DNA.¹⁵⁸ (B) A label-free linear probe prevents a redox label from interacting with the electrode in the absence of a target DNA, while is degraded by the enzyme upon hybridization to the target.¹⁶⁸

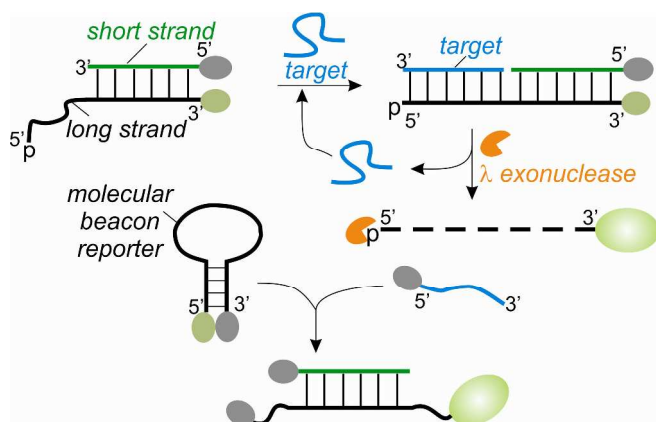


Fig. 30. Fluorescent DNA detection using a double-stranded probe.¹⁶⁹

A homogeneous fluorescent assay was reported by Liu and colleagues.¹⁶⁹ The assay made use of a fluorophore and a quencher-labeled partial DNA duplex with a 5'-phosphorylated long strand as a probe (Fig. 30). The proximity of the fluorophore to the quencher in the duplex ensured low fluorescence. In the absence of a DNA target the 5'-phosphorylated fragment of the duplex was in a single stranded form, which prevented the phosphorylated probe from cleavage by λ exonuclease. When the target hybridized to the single-stranded fragment of

the duplex probe, it formed a substrate for the enzyme. As a result of enzymatic digestion, the fluorophore, the target and the short strand were released in solution. Fluorescent signal increased. To further increase the signal, the released short strand opened an MB reporter, thus (Fig. 30, bottom). The authors reported the LOD of 68 fM and good selectivity of the assay.

A split probe was used for a λ exonuclease-assisted assay producing a surface enhanced Raman scattering (SERS) signal (*exo*-SERS approach).¹⁷⁰ It contained a 3'-biotinylated capture oligonucleotide and a 5'-phosphorylated reporter probe carrying a TAMRA label attached to its 3'-end via a hexaethylene glycol-containing decaadenylate linker (Fig. 31). The linker was essential to facilitate SERS signal. Both the capture and reporter probes were complementary to the adjacent positions of a target DNA. The probe-target complex was separated from the excess of the reporter probe using streptavidin-coated magnetic beads. This complex contained a 5'-phosphate at the reporter and was digested by λ exonuclease resulting in the release of a TAMRA-labeled short fragment, which produced the characteristic TAMRA-related SERS signal. Using the assay, an 85-bp PCR fragment of the *ompA* gene of *Chlamydia trachomatis* was detected with a LOD of 77 pM. High selectivity of the assay allowed differentiation between the specific target and a non-specific PCR fragment from *C. glabrata*.

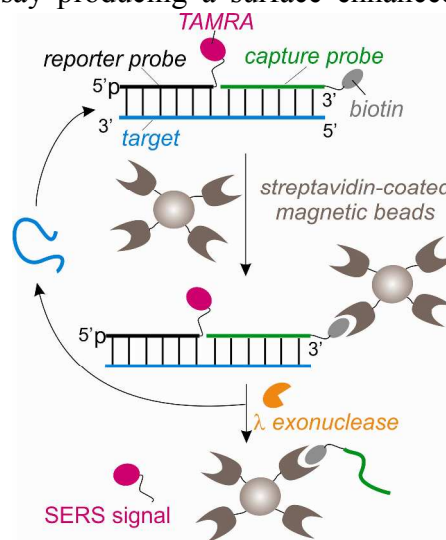


Fig. 31. *exo*-SERS approach.¹⁷⁰

4.3. RNase H-assisted assays

RNase H degrades the RNA strand in DNA/RNA duplexes. The enzyme does not cleave unhybridized RNA, as well as both single- and double-stranded DNA.¹⁷¹ It is a non-specific endonuclease, which catalyzes hydrolysis of RNA phosphodiester bonds. The cleavage products contain 3'-hydroxyl and 5'-phosphate groups.

RNase H was used for a signal amplification approach named “cycling probe technology” (CPT).¹⁷² In this isothermal approach with linear signal amplification, a chimeric probe made of DNA with an insert of ribonucleotides was utilized (Fig. 32A). The probe was found to require at least four ribonucleotides for efficient cleavage by RNase H.¹⁷³ RNase H cleaved within the RNA portion of the probe in the probe-target hybrid, and the probe fragments dissociated from the complex. The fragments of the probe are accumulated providing the means for the target detection by a number of techniques (Fig. 32B). Originally, a CPT assay with a [γ -³²P]-labeled chimeric probe was developed for the gel-based detection of the direct repeat region in *Mycobacterium tuberculosis*.¹⁷⁴ The assay demonstrated good specificity and was able to differentiate between genomic DNA from *M. tuberculosis* and six species of nontuberculous mycobacteria. A lower LOD corresponded to 100 bacterial cells. The authors reported that roughly 1000 cleavage events occur within 30-min of the reaction.

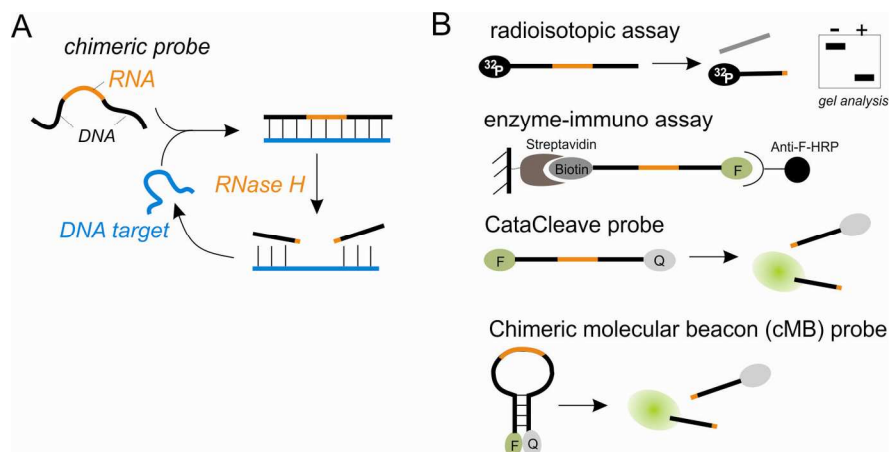


Fig. 32. Cycling probe technology (CPT). (A) The principle of CPT. (B) Different formats of CPT-based assays.

In its later variations, CPT was combined with an enzyme-immuno assay (EIA) for colorimetric detection.¹⁷⁵⁻¹⁷⁸ The chimeric probe was labeled with fluorescein and biotin at its 5'- and 3'-ends, respectively (Fig. 32B). After sufficient rounds of RNase H-catalyzed probe cleavage, the uncleaved probe was captured by surface-immobilized streptavidin and detected using anti-fluorescein antibodies conjugated with horseradish peroxidase. CPT-EIA assays were developed for the detection of the *mecA* gene in methicillin-resistant *Staphylococcus aureus*,¹⁷⁵⁻¹⁷⁷ *vanA* and *vanB* genes in vancomycin-resistant enterococci.¹⁷⁸

Non-radioactive detection of *Mycobacterium tuberculosis* complex (MTC) bacterial species using CPT was achieved.¹⁷⁹ A 5'-biotinylated chimeric probe targeted Mt308 fragment, which is present as a single copy in the species belonging to MTC. The probe was cleaved by RNase H in the probe-target hybrid producing two fragments. The biotin-labeled fragment was complementary to a capture probe immobilized on the surface of a microplate well. After washing, the immobilized duplex was colorimetrically detected using a streptavidin peroxidase conjugate. Due to steric hindrance, the longer uncleaved chimeric probe could not efficiently hybridize to the capture probe, providing a basis for the detection. The LOD of the assay was found to be 1 pM for a synthetic DNA target.

An alternative method for separation/detection in a CPT assay using capillary gel electrophoresis with laser-induced fluorescence (CGE-LIF) was reported by Dickinson et al.¹⁸⁰ It was shown that CGE-LIF CPT assay could be completed within about 1 h with less than 4 min required for the separation/detection step, while total time for the radioisotopic PAGE CPT assay was 3-12 h. The LOD of 10^5 - 10^6 copies of genomic DNA from *Erwinia herbicola* was achieved with both CGE-LIF and radioisotopic PAGE methods. Another CPT assay for the detection of the *mecA* gene of MRSA employed a microfluidic chip with gel-free capillary electrophoresis separation of the chimeric probe fragments.¹⁸¹ With off-chip CPT and on-chip separation/detection, the LOD of 2 fM for the detection of a *mecA*-related 29-mer single-stranded DNA analyte was reported. A fluorescent CPT-based DNA detection was demonstrated using a CataCleave probe, a chimeric probe containing two different fluorophores (FAM and TAMRA) adjacent to the 5' and 3'-ends of the RNA insert (Fig. 32B).¹⁸² The CataCleave probe targeting the *capC* gene of *Bacillus anthracis* detected 10 nM synthetic oligonucleotide in 5 min. When combined with RCA, the probe was capable of real-time detection of 0.6 pM analyte.

RNase H-dependent signal amplification strategy with fluorescent readout was also employed with a chimeric molecular beacon (cMB) probe.^{183,184} In this case the loop fragment of the DNA MB probe was made of ribonucleotides. The RNA portion of cMB probe in the probe-

target complex was cleaved by RNase H. The cleavage released the target and separated the fluorophore-containing cMB fragment from the quencher, thus increasing the fluorescence of the solution. Unfortunately, the LOD of these assays was not reported, but 100 pM DNA target was shown to trigger about 8-fold fluorescence increase over the background.¹⁸⁴ Other reports described an assay with an SNP-specific cMB probe carrying a single ribonucleotide insert.^{185,186} When bound to a complementary DNA target, this probe was cleaved at the 5'-side of the ribonucleotide by RNase HIII from either *Chlamidia pneumonia*¹⁸⁵ or *Thermus thermophilus*.¹⁸⁶ In comparison with a simple MB-based hybridization assay, a 90-fold enhancement in fluorescence change was observed.¹⁸⁵ For SNPs differentiation the probe was designed to have the ribonucleotide insert complementary to -1 or +1 position from the SNP site.¹⁸⁶ The enzyme could not cleave the mismatched duplexes, thus providing the means for SNP differentiation. With this approach, about 200 pM dsDNA target could be detected under thermal cycle conditions. Two allele-specific cMB probes were required to genotype each SNP site.

Indirect binding of the cMB probe with an analyzed target in RNase HIII-assisted assay enabled to use a single cMB probe for both alleles.⁸⁵ In this report, the cMB probe containing two single ribonucleotide inserts was used in conjunction with two DNA adaptor strands, each of which contained a fragment complementary to the cMB probe and a fragment complementary to the DNA or RNA analytes (Fig. 33). In the presence of the analyte, a 4J tetrapartite complex containing the adaptor strands, the analyte and the cMB probe was formed. The cMB probe in the complex was cleaved by RNase HIII into three fragments, which resulted in destabilization of the complex and consequent release of the adaptor strands and the target for next round of probe recognition and cleavage.

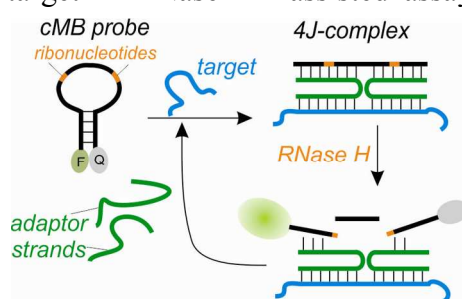


Fig. 33. Indirect binding of a cMB probe to a target using a 4J structure.⁸⁵

The approach is applicable for both DNA and RNA analysis, since RNase HIII employed for signal amplification preferably cleaves double-stranded DNA with a single ribonucleotide insert, while is less efficient in cleavage of RNA/DNA hybrids. The LOD of 300 pM for a synthetic analyte mimicking a fragment of hepatitis C virus (HCV) mRNA was demonstrated. Exceptionally high selectivity of the approach that enabled differentiation between two alleles of human SNP rs717302 at room temperature was achieved due to the binary character of the hybridization probe.²¹ Both HCV RNA and rs717302 analytes were detected using the same cMB probe and the adaptor strands with the analyte-specific fragments.

RNase-H assisted target recycling was described for linear RNA probes.¹⁸⁷⁻¹⁸⁹ According to one approach, the label-free probes were arranged in microarrays.^{187,188} In the presence of specific DNA targets, the target-bound probes were degraded by RNase H, and the signal was detected using surface plasmon resonance imaging. The assay enabled a PCR-free detection of the TSPY gene in human genomic DNA with the LOD of 1 fM.¹⁸⁸ In another approach, the probe was modified with gold nanoparticles and a fluorescein label at its 5'- and 3'-ends, respectively.¹⁸⁹ The proximity of the dye to the gold nanoparticle quenched its fluorescence ensuring low signal in the absence of a target DNA. When, the probe hybridized to the target, the RNA-DNA probe-target hybrid became a substrate for the enzyme, which cleaved the probe releasing the fluorophore in solution. The target DNA at 10 pM concentration triggered 1.8-fold increase.

Overall, RNase H requires synthesis of ribonucleotide-containing reporter oligonucleotide, which are more expensive than DNA probes required for alternative EATR approaches. However these probes can be used as universal reporters for both DNA and RNA analytes of any sequence.

4.4. AP endonuclease-assisted assays

Some EATR-based nucleic acid assays made use of a linear dual-labeled probe containing an apurinic/apyrimidinic (AP) sites (AP probes) and a catalytic action of AP endonuclease.^{190,191} AP endonuclease catalyzes cleavage of the phosphodiester bonds 3' and 5' to the AP site.¹⁹² The probe was able to detect as little as 10 fmol of a synthetic target, which corresponds to 0.2 nM target in solution.¹⁹⁰ The approach was adopted for the detection of active transcription factors by utilizing an AP probe containing a consensus binding sequence.¹⁹¹ An AP probe containing the E-box consensus sequence could detect the functional heterodimer of the transcription factors CLOCK/BMAL1, which are a major component of the biological clock system, from as few as 3000 HeLa cells.

4.5. Duplex-specific nuclease-assisted assays

Duplex-specific nuclease (DSN) catalyzes DNA cleavage in DNA/DNA and RNA/DNA duplexes, while it renders inactive on single-stranded DNA and RNA.¹⁹³ It requires perfectly matched duplexes of 8-12 bp in length. Strong preference of the enzyme to double-stranded nucleic acids makes it attractive for EATR-based assays. DSN signal amplification (DSNSA) approach was used for microRNA detection with either a dual-labeled probe¹⁹⁴ or a hairpin probe.^{195,196} The LOD of 0.1 pM was reported for the dual-labeled probe assay, which is comparable with PCR-based assays for microRNA detection. For the MB probe-dependent fluorescent assay the LOD of 0.4 pM was demonstrated.¹⁹⁵ In this assay, the stem of the MB probe was made of 2-*O*-methyl ribonucleotides to prevent the probe from the background DSN-catalyzed cleavage. The high selectivity of both assays allowed discrimination between the closely related target sequences belonging to the same microRNA family. In yet another DSN-assisted target recycling assay with fluorescent readout, the hairpin probe contained a sequence of deoxyribozyme 8-17, which was partially sequestered in the stem and, therefore, inactive.¹⁹⁶ DSN-catalyzed cleavage of the probe in the probe-target complex liberated the active deoxyribozyme 8-17, which could then bind and cleave a MB reporter, thus producing fluorescent signal. Working together, DSN and 8-17 constituted a dual cascade signal amplification system. Unfortunately, the detection limit of the system was only 10 pM, which was disadvantageous in comparison with the non-cascading fluorescent assays.

Another variation of the same hairpin probe was developed for visual or colorimetric readout.¹⁹⁶ Instead of 8-17 sequence, the probe contained the sequence for peroxidase-like G-quadruplex deoxyribozyme. The G-rich sequence of the deoxyribozyme was partially complementary with the 5'-terminal fragment of the hairpin forming an 8-nt "interfering tail". The rest of the G-rich sequence remained single-stranded at the 3'-end of the probe. Enzymatic cleavage of the probe in the presence of the target liberated the active G-quadruplex. As a result, green color of the solution was produced in the presence of hemin, ABTS and H₂O₂. It was found that a visual color change could be detected in the presence of as low as 2 nM target microRNA. At the same time, the use of a UV/Vis-spectrometer allowed detection down to 20-80 pM target.

4.6. DNase I-assisted assays

DNase I is an endonuclease with a broad specificity. It catalyzes phosphodiester bond cleavage in DNA utilizing single- or double-stranded DNA or DNA/RNA hybrids as substrates. The products of DNase I-catalyzed cleavage are di-, tri- and oligonucleotides with 5'-phosphates and 3'-hydroxyl groups.¹⁹⁷ Since the enzyme is not active towards RNA hydrolysis, it was used in EATR assays for microRNA detection. *In fact, DNase I assays are limited to RNA detection, since a DNA target would be cleaved by the enzyme along with the probe. Another limitation of DNase I-assisted assays is that an additional component capable of protecting the probe from the enzyme-dependent cleavage in the absence of the target is required.* For this purpose, nanomaterials were suggested. For instance, GO is known to efficiently absorb single-stranded DNA and protect it from DNase I action.¹⁹⁸ In the assay developed by Yang and co-authors,¹⁹⁹ a fluorophore-labeled single-stranded probe was constrained from enzyme-catalyzed cleavage by interacting with GO in the absence of a microRNA target. GO also serves as a quencher of the fluorescent label, keeping the background low. If present, the target hybridized to the probe, which weakened the probe-target complex interactions with GO. As a result, the probe in the complex was degraded by DNase I, while the microRNA target remained intact and could subsequently bind another probe molecule. The released fluorophore was separated from the quencher enabling high fluorescent signal. The assay could be employed in a multiplex format due to the ability of GO to efficiently quench fluorescence of a broad range of fluorophores. A linear correlation between the signal and the target concentration was reported in the range of 20 pM-1 nM, with the detection limit of 9 pM. In addition, excellent differentiation between the closely related sequences of microRNAs was demonstrated.

4.7. T7 exonuclease-assisted assays

Another enzyme employed for an EATR strategy is T7 exonuclease, which catalyzes stepwise removal of mononucleotides from the 5'-end of a double-stranded DNA. It was used with a dual-labeled probe bearing a fluorophore on its 5'-end and a quencher three nucleotides away from the fluorophore.²⁰⁰ The probe targeted the telomeric repeat sequence and, therefore, enabled detection of telomerase activity, which adds the repeats onto the 3'-end of the human chromosomes. However, the same principle can be employed to any nucleic acid sequence of interest by designing the correspondent sequence-specific probe. The strategy was named “T7 exonuclease-assisted target recycling amplification” (TEATR). The telomerase assay utilized a primer that became elongated with the repeat sequences by the action of telomerase to produce a target for the probe recognition. T7 exonuclease cleaved off the end fluorophore label of the probe in the probe-target complex, resulting in its separation from the quencher and fluorescence increase. The target remained intact due to the 5'-terminal “overhang”. Upon degradation of the probe, the target was released from the probe-target complex to be able to bind a new probe molecule. The limit of detection of telomerase activity was equivalent to as few as 5 HeLa cells. The assay was also useful for screening telomerase inhibitors.

Conclusion

Providing linear, not exponential, amplification, EATR approaches tend to have higher LODs than PCR. However, the versatility and the potential to generate visual output signal make EATR promising for point-of-care diagnostics of diseases in the future. The EATR assays described in this review vary in terms of both the type of the oligonucleotide reporters and the enzyme used

for signal amplification. These assays can be grouped into simple assays, which use only EATR strategy for signal amplification, and composite assays, which take advantage of additional strategies for improving LODs. The additional strategies include SDA or RCA to amplify the amount of the detected sequences (not necessary the original targets that initiate the dual amplification process), as well as formation of super-sandwich-like structures in case of electrochemical assays. The composite assays typically enable lower LODs, which in some reports are as low as 20 aM. This LOD corresponds to 1200 molecules in a 100- μ L sample and is comparable with that of PCR. Most of the reported LODs, however, were obtained for synthetic targets in artificial systems and have not been validated for clinical or environmental samples. On the other hand, the multicomponent and multistage composite assays are potentially harder to optimize and reproduce, which may impact the assay robustness and increase the rate of false-positive and false-negative results. Multistage assays would also require longer hands-on time and more reagents.

A possible limitation of EATR-based approaches is less efficient activity of enzymes with oligonucleotide substrates covalently attached to a solid support. This should be taken into account when heterogeneous assays (e.g. electrode- or nanoparticle-based formats) are designed. In this case, the EATR reaction should preferably be completed in solution prior to analysis of the cleavage products.

Taking in consideration the advantages and limitations of EATR it is important to identify the most useful applications for this class of techniques. Simple EATR-based assays are unlikely to be competitive with PCR-based techniques in molecular diagnostics in terms of sensitivity. A possible niche of EATR is in point-of-care (POC) diagnostics, where robust, inexpensive and easy-to-use diagnostic tests are required. Indeed, many EATRs described above can operate in mix-and-read formats and produce signals that can be detected without the need of expensive equipment. The POC tests should preferably avoid multiple manipulation steps and long incubation time, as well as minimize equipment use, which creates a venue towards further optimization and perfection of EATR.

Another possible application of EATR-based approaches (especially, ones operating via dual amplification) is SNP genotyping, where they appear to be competitive with rtPCR in terms of selectivity. SNP-specific real-time PCR technologies require expensive reagents and PCR thermal cyclers that can measure melting curves. Indeed, some of the aforementioned EATR assays demonstrate great selectivity in the analysis of single-base substitutions owing to either the sensitivity of the cleaving enzymes to mismatches or the split or conformationally-constrained probe design. Importantly, the high selectivity is achieved at ambient temperatures, which does not require time consuming and expensive analysis of melting temperatures. For an EATR technique to be especially useful in SNP genotyping, it should be label-free or use the same labeled reporter for multiple targets. Such EATR technologies are already available.

Third application niche is in the field of microRNA detection, which receives growing attention due to the importance of microRNA for early stage cancer diagnostics. MicroRNA targets represent a challenge for conventional PCR and other primer-dependent target amplification techniques due to their short length (22-25 nt). EATR-based approaches are compatible with the detection of short nucleotide sequences. Indeed, we mentioned a number of EATR reports with the detection level of microRNA ranging from 0.5 fM to 20 pM. However, to be applicable in this field, the assay must use only the enzyme that processes DNA/RNA hybrids as substrates. This requirement limits the use of RNases, nicking endonucleases, and flap endonucleases. At the same time, such limitation can be overcome if a “smart” design of the

probe is employed. An example of such design is indirect binding of the cleavable reporter to the analyzed target sequence.

In general, EATR is a perspective strategy for nucleic acid detection. However, the future of the field depends on how significant are the reported proof-of-concept designs in real diagnostic settings with clinical samples. A history of a commercialized PCR-free EATR technique, the Invader assay, illustrates the importance and challenges of EATR technology for practical applications, which should be taken in account when new EATR test is designed.

References

1. M. S. Cordray and R. R. Richards-Kortum, *Am. J. Trop. Med. Hyg.*, 2012, **87**, 223-230.
2. F. Ahmad and S. A. Hashsham, *Anal. Chim. Acta*, 2012, **733**, 1-15.
3. L. M. Feazel, D. N. Frank, V. R. Ramakrishnan, *Int. Forum Allergy Rhinol.*, 2011, **1**, 451-459.
4. M. de Planell-Saguer and M. C. Rodicio, *Clin. Biochem.*, 2013, **46**, 869-878.
5. H. Sandhu and H. Maddock, *Clin. Sci.*, 2014, **126**, 377-400.
6. A. Fendler and K. Jung, *Crit. Rev. Oncog.*, 2013, **18**, 289-302.
7. S. Sforza, R. Corradini, T. Tedeschi, R. Marchelli, *Chem. Soc. Rev.*, 2011, **40**, 221-232.
8. M. Miraglia, K. G. Berdal, C. Brera, P. Corbisier, A. Holst-Jensen, E. J. Kok, H. J. Marvin, H. Schimmel, J. Rentsch, J. P. van Rie, J. Zagon, *Food Chem. Toxicol.*, 2004, **42**, 1157-1180.
9. L. Nicoloso, P. Crepaldi, R. Mazza, P. Ajmone-Marsan, R. Negrini, *Recent Pat. Food Nutr. Agric.*, 2013, **5**, 9-18.
10. R. G. Dumitrescu, *Methods Mol. Biol.*, 2012, **863**, 3-14.
11. H. Jang and H. Shin, *World J. Gastroenterol.*, 2013, **19**, 1030-1039.
12. M. Hassanein, J. C. Callison, C. Callaway-Lane, M. C. Aldrich, E. L. Grogan, P. P. Massion, *Cancer Prev. Res.*, 2012, **5**, 992-1006.
13. M. Bauer, *Forensic Sci. Int. Genet.*, 2007, **1**, 69-74.
14. G. Meakin and A. Jamieson, *Forensic Sci. Int. Genet.*, 2013, **7**, 434-443.
15. E. Giardina, A. Spinella, G. Novelli, *Nanomedicine*, 2011, **6**, 257-270.
16. D. A. Ray, J. A. Walker, M. A. Batzer, *Mutat. Res.*, 2007, **616**, 24-33.
17. Y. Y. Wu and G. Csako, *Clin. Chim. Acta*, 2006, **363**, 165-176.
18. T. Yasui, N. Kaji, Y. Baba, *Annu. Rev. Anal. Chem.*, 2013, **6**, 83-96.
19. R. A. Cardullo, S. Agrawal, C. Flores, P. C. Zamecnik, D. E. Wolf, *Proc. Natl. Acad. Sci. USA*, 1988, **85**, 8790-8794.
20. K. Ebata, M. Masuko, H. Ohtani, M. Kashiwasake-Jibu, *Photochem. Photobiol.*, 1995, **62**, 836-839.
21. D. M. Kolpashchikov, *Chem. Rev.*, 2010, **110**, 4709-4723.
22. S. Tyagi, F. R. Kramer, *Nat. Biotechnol.*, 1996, **14**, 303-308.
23. D. M. Kolpashchikov, *Scientifica*, 2012; **2012**, 928783.
24. W. Tan, K. Wang, T. J. Drake, *Curr. Opin. Chem. Biol.*, 2004, **8**, 547-553.
25. Q. Wang, L. Chen, Y. Long, H. Tian, J. Wu, *Theranostics*, 2013, **3**, 395-408.

26. A. M. Blanco and R. A. Artero, *Methods*, 2010, **52**, 343-351.
27. B. Juskowiak, *Anal. Bioanal. Chem.*, 2011, **399**, 3157-3176.
28. G. Schochetman, C. Y. Ou, W. K. Jones, *J. Infect. Dis.*, 1988, **158**, 1154-1157.
29. M. Botes, M. de Kwaadsteniet, T. E. Cloete, *Anal. Bioanal. Chem.*, 2013, **405**, 91-108.
30. L. S. Kristensen and L. L. Hansen, *Clin. Chem.*, 2009, **55**, 1471-1483.
31. R. F. Medrano and C. A. de Oliveira, *Mol. Biotechnol.*, 2014, DOI 10.1007/s12033-014-9734-4
32. M. Fakruddin, K. S. Mannan, A. Chowdhury, R. M. Mazumdar, M. N. Hossain, S. Islam, M. A. Chowdhury, *J. Pharm. Bioapplied Sci.*, 2013, **5**, 245-252.
33. P. Gill and A. Ghaemi, *Nucleosides Nucleotides Nucleic Acids*, 2008, **27**, 224-243.
34. P. Craw and W. Balachandran, *Lab. Chip*, 2012, **12**, 2469-2486.
35. J. Kim and C. J. Easley, *Bioanalysis*, 2011, **3**, 227-239.
36. D. Andresen, M. von Nickisch-Rosenegk, F. F. Bier, *Expert Rev. Mol. Diagn.*, 2009, **9**, 645-650.
37. Y. J. Jeong, K. Park, D. E. Kim, *Cell Mol. Life Sci.*, 2009, **66**, 3325-3336.
38. G. T. Walker, M. S. Fraiser, J. L. Schram, M. C. Little, J. G. Nadeau, D. P. Malinowski, *Nucleic Acids Res.*, 1992, **20**, 1691-1696.
39. E. T. Han, *Expert Rev. Mol. Diagn.*, 2013, **13**, 205-218.
40. Y. Mori and T. Notomi, *J. Infect. Chemother.*, 2009, **15**, 62-69.
41. T. Notomi, H. Okayama, H. Masubuchi, T. Yonekawa, K. Watanabe, N. Amino, T. Hase, *Nucleic Acids Res.*, 2000, **28**, E63.
42. M. Parida, S. Sannarangaiah, P. K. Dash, P. V. Rao, K. Morita, *Rev. Med. Virol.*, 2008, **18**, 407-421.
43. Z. K. Njiru, *PLoS Negl. Trop. Dis.*, 2012, **6**, e1572.
44. S. Santiago-Felipe, L. A. Tortajada-Genaro, R. Puchades, A. Maquieira, *Anal. Chim. Acta*, 2014, **811**, 81-87.
45. A. A. E. Wahed, P. Patel, D. Heidenreich, F. T. Hufert, M. Weidmann, *PLoS Curr.*, 2013, **Dec 12**.
46. W. Zhao, M. M. Ali, M. A. Brook, Y. Li, *Angew. Chem. Int. Ed. Engl.*, 2008, **47**, 6330-6337.
47. M. Stougaard, S. Juul, F. F. Andersen, B. R. Knudsen, *Integr. Biol.*, 2011, **3**, 982-992.
48. W. Zhao, M. M. Ali, M. A. Brook, Y. Li, *Angew. Chem. Int. Ed.*, 2008, **47**, 6330-6337.
49. V. V. Demidov, *Expert Rev. Mol. Diagn.*, 2002, **2**, 542-548.
50. T. Kobori and H. Takahashi, *Anal. Sci.*, 2014, **30**, 59-64.
51. M. L. Collins, B. Irvine, D. Tyner, E. Fine, C. Zayati, C. Chang, T. Horn, D. Ahle, J. Detmer, L.-P. Shen, J. Kolberg, S. Bushnell, M. S. Urdea, D. D. Ho, *Nucleic Acids Res.*, 1997, **25**, 2979-2984.
52. G. J. Tsongalis, *Am. J. Clin. Pathol.*, 2006, **126**, 448-453.
53. R. M. Dirks and N. A. Pierce, *Proc. Natl. Acad. Sci.*, 2004, **101**, 15275-15278.
54. Z. Ge, M. Lin, P. Wang, H. Pei, J. Yan, J. Shi, Q. Huang, D. He, C. Fan, X. Zuo, *Anal. Chem.*, 2014, **86**, 2124-2130.

55. F. M. Spiga, A. Bonyár, B. Ring, M. Onofri, A. Vinelli, H. Sántha, C. Guiducci, G. Zuccheri, *Biosens. Bioelectron.*, 2014, **54**, 102-108.
56. E. J. Speel, A. H. Hopman, P. Komminoth, *Methods Mol. Biol.*, 2006, **326**, 33-60.
57. K. Y. Chumbimuni-Torres, J. Wu, C. Clawson, M. Galik, A. Walter, G.-U. Flechsig, E. Bakker, L. Zhang, J. Wang, *Analyst*, 2010, **135**, 1618-1623.
58. Q. Li and B. J. Boyd, *Analyst*, 2013, **138**, 391.
59. J. Xu, J. Jiang, J. Su, Y. Xiang, R. Yuan, Y. Chai, *Chem. Commun.*, 2012, **48**, 3309-3311.
60. E. D. Goluch, S. I. Stoeva, J. S. Lee, K. A. Shaikh, C. A. Mirkin, C. Liu, *Biosens. Bioelectron.*, 2009, **24**, 2397-2403.
61. C. P. Chan, *Bioanalysis*, 2009, **1**, 115-133.
62. S. H. Um, J. B. Lee, S. Y. Kwon, Y. Li, D. Luo, *Nat. Protoc.*, 2006, **1**, 995-1000.
63. C. S. Thaxton, D. G. Georganopoulou, C. A. Mirkin, *Clin. Chim. Acta*, 2006, **363**, 120-126.
64. Lee J. B., Campolongo M. J., Kahn J. S., Roh Y. H., Hartman M. R., Luo D., *Nanoscale*, 2010, **2**, 188-197.
65. S. C. Andras, J. B. Power, E. C. Cocking, M. R. Davey, *Mol. Biotechnol.*, 2001, **19**, 29-44.
66. J. Lei and H. Ju, *Chem. Soc. Rev.*, 2012, **41**, 2122-2134.
67. A. Chen and S. Chatterjee, *Chem. Soc. Rev.*, 2013, **42**, 5425-5438.
68. M. R. Hartman, R. C. H. Ruiz, S. Hamada, C. Xu, K. G. Yancey, Y. Yu, W. Han, D. Luo, *Nanoscale*, 2013, **5**, 10141-10154.
69. C. S. Thaxton, D. G. Georganopoulou, C. A. Mirkin, *Clin. Chim. Acta*, 2006, **363**, 120-126.
70. M. M.-C. Cheng, G. Cuda, Y. L. Bunimovich, M. Gaspari, J. R. Heath, H. D. Hill, C. A. Mirkin, A. J. Nijdam, R. Terracciano, T. Thundat, M. Ferrari, *Curr. Opin. Chem. Biol.*, 2006, **10**, 11-19.
71. P. M. Holland, R. D. Abramson, R. Watson, D.H. Gelfand, *Proc. Natl. Acad. Sci. USA*, 1991, **88**, 7276-7280.
72. C. A. Heid, J. Stevens, K. J. Livak, P. M. Williams, *Genome Res.*, 1996, **6**, 986-994.
73. V. Lyamichev, A. L. Mast, J. G. Hall, J. R. Prudent, M. W. Kaiser, T. Takova, R.W. Kwiatkowski, T. J. Sander, M. de Arruda, D. A. Arco, B. P. Neri, M. A. Brow, *Nat. Biotechnol.*, 1999, **17**, 292-296.
74. R. W. Kwiatkowski, V. Lyamichev, M. de Arruda, B. Neri, *Mol. Diagn.*, 1999, **4**, 353-364.
75. M. Olivier, *Mutat. Res.*, 2005, **573**, 103-110.
76. L. G. Lee, C. R. Connell, W. Bloch, *Nucleic Acids Res.*, 1993, **21**, 3761-3766.
77. K. J. Livak, S. J. Flood, J. Marmaro, W. Giusti, K. Deetz, *PCR Methods Applic.*, 1995, **4**, 357-362.
78. C.-H. Lu, H.-H. Yang, C.-L. Zhu, X. Chen, G.-N. Chen, *Angew. Chem. Int. Ed.*, 2009, **48**, 4785-4787.
79. Y. Wang, Z. Li, J. Wang, J. Li, Y. Lin, *Trends Biotechnol.*, 2011, **29**, 205-212.
80. N. Varghese, U. Mogera, A. Govindaraj, A. Das, P.K. Maiti, A.K. Sood, C.N. Rao, *Chemphyschem*, 2009, **10**, 206-210.
81. L. Zhang, C. Z. Huang, Y. F. Li, S.J. Xiao, J.P. Xie, *J. Phys. Chem.*, 2008, **112**, 7120-7122.
82. H. Li, Y. Zhang, L. Wang, J. Tian, X. Sun, *Chem. Commun.*, 2011, **47**, 961-963.
83. Y. Xiao, B. D. Piorek, K. W. Plaxco, A. J. Heeger, *J. Am. Chem. Soc.*, 2005, **125**, 17990-17991.
84. S. Nakayama, L. Yan, H.O. Sintim, *J. Am. Chem. Soc.*, 2008, **130**, 12560-12561.
85. Y. V. Gerasimova, S. Peck, D. M. Kolpashchikov, *Chem. Commun.*, 2010, **46**, 8761-8763.

86. D. Sen, W. Gilbert, *Nature*, 1988, **334**, 364-366.
87. P. Travascio, Y.F. Li, D. Sen, *Chem. Biol.*, 1998, **5**, 505-517.
88. B. T. Roembke, S. Nakayama, H. O. Sintim, *Methods*, 2013, **64**, 185-198.
89. K.-J. Jang, H. Lee, H.-L. Jin, Y. Park, J.-M. Nam, *Small*, 2009, **23**, 2665-2668.
90. S. Liu, Y. Hu, J. Jin, H. Zhang, C. Cai, *Chem. Commun.*, 2009, **45**, 1635-1637.
91. S. Liu, P. Wu, W. Li, H. Zhang, C. Cai, *Anal. Chem.*, 2011, **83**, 4752-4758.
92. D. Tang, J. Tang, B. Su, Q. Li, G. Chen, *Chem. Commun.*, 2011, **47**, 9477-9479.
93. Y. Fei, X.-Y. Jin, Z.-S. Wu, S.-B. Zhang, G. Shen, R.-Q. Yu, *Anal. Chim. Acta*, 2011, **691**, 95-102.
94. L. Yan, S. Nakayama, S. Yitbarek, I. Greenfield, H.O. Sintim, *Chem. Commun.*, 2011, **47**, 200-202.
95. L. Yan, S. Nakayama, H.O. Sintim, *Bioorg. Med. Chem.*, 2013, **21**, 6181-6185.
96. Q. Wang, L. Yang, X. Yang, K. Wang, L. He, J. Zhu, T. Su, *Chem. Commun.*, 2012, **48**, 2982-2984.
97. Z. Shen, S. Nakayama, S. Semancik, H.O. Sintim, *Chem. Commun.*, 2012, **48**, 7580-7582.
98. Z. Zhu, F. Gao, J. Lei, H. Dong, H. Ju, *Chem. Eur. J.*, 2012, **18**, 13871-13876.
99. Y. Weizmann, Z. Cheglakov, V. Pavlov, I. Willner, *Angew. Chem. Int. Ed.*, 2006, **45**, 2238-2242.
100. D. A. Wah, J. Bitinaite, I. Schildkraut, A. K. Aggarwal, *Proc. Natl. Acad. Sci. USA*, 1998, **95**, 10564-10569.
101. S. H. Chan, B. L. Stoddard, S. Y. Xu, *Nucleic Acids Res.*, 2011, **39**, 1-18.
102. T. Kiesling, K. Cox, E. A. Davidson, K. Dratchen, G. Grater, S. Hibbard, R. S. Lasken, J. Leshin, E. Skowronski, M. Danielsen, *Nucleic Acids Res.*, 2007, **35**, e117.
103. W. Gao, X. Li, L. Zeng, T. Peng, *Diagn. Microbiol. Infect. Dis.*, 2008, **60**, 133-141.
104. S. Niu, Q. Li, L. Qu, W. Wang, *Anal. Chim. Acta*, 2010, **680**, 54-58.
105. Y. Song, W. Li, Y. Duan, Z. Li, L. Deng, *Biosens. Bioelectron.*, 2014, **55**, 400-404.
106. J. J. Li, Y. Chu, B. Y.-H. Lee, X. S. Xie, *Nucleic Acids Res.*, 2008, **36**, e36.
107. R.-M. Kong, X.-B. Zhang, L.-L. Zhang, Y. Huang, D.-Q. Lu, W. Tan, G.-L. Shen, R.-Q. Yu, *Anal. Chem.*, 2011, **83**, 14-17.
108. H. Dong, K. Hao, Y. Tian, S. Jin, H. Lu, S.-F. Zhou, X. Zhang, *Biosens. Bioelectron.*, 2014, **53**, 377-383.
109. G. Wang and C. Zhang, *Anal. Chem.*, 2012, **84**, 7037-7042.
110. G. Zhu, K. Yang, C. Zhang, *Biosens. Bioelectron.*, 2013, **49**, 170-175.
111. B.-C. Yin, Y.-Q. Liu, B.-C. Ye, *Anal. Chem.*, 2013, **85**, 11487-11493.
112. B. Zou, Y. Ma, H. Wu, G. Zhou, *Angew. Chem. Int. Ed.*, 2011, **50**, 7395-7398.
113. Z. Lin, W. Yang, G. Zhang, Q. Liu, B. Qiu, Z. Cai, G. Chen, *Chem. Commun.*, 2011, **47**, 9069-9071.
114. J. Li, Q.-H. Yao, H.-E. Fu, X.-L. Zhang, H.-H. Yang, *Talanta*, 2011, **85**, 91-96.
115. Y. Xiao, V. Pavlov, T. Niazov, A. Dishon, M. Kotler, I. Willner, *J. Am. Chem. Soc.*, 2004, **126**, 7430-7431.
116. B. T. Roembke, S. Nakayama, H. O. Sintim, *Methods*, 2013, **64**, 185-198.
117. S. Bi, Y. Cui, L. Li, *Anal. Chim. Acta*, 2013, **760**, 69-74.
118. C. Yan, C. Jiang, J. Jiang, R. Yu, *Anal. Sci.*, 2013, **29**, 605-610.
119. J. Chen, J. Zhang, J. Li, F. Fu, H.-H. Yang, G. Chen, *Chem. Commun.*, 2010, **46**, 5939-5941.
120. Z. Liu, W. Zhang, S. Zhu, L. Zhang, L. Hu, *Biosens. Bioelectron.*, 2011, **29**, 215-218.

121. Y. Chen, Q. Wang, J. Xu, Y. Xiang, R. Yuan, Y. Chai, *Chem. Commun.*, 2013, **49**, 2052-2054.
122. H. Zhou, Y.-Y. Zhang, J. Liu, J.-J. Xu, H.-Y. Chen, *Chem. Commun.*, 2013, **49**, 2246-2248.
123. S. Bi, J. Zhang, S. Zhang, *Chem. Commun.*, 2010, **46**, 5509-5511.
124. J. Chen, J. Zhang, Y. Guo, J. Li, F. Fu, H.H. Yang, G. Chen, *Chem. Commun.*, 2011, **47**, 8004-8006.
125. H. Ji, F. Yan, J. Lei, H. Ju, *Anal. Chem.*, 2012, **84**, 7166-7171.
126. Q. Wang, C. Yang, Y. Xiang, R. Yuan, Y. Chai, *Biosens. Bioelectron.*, 2014, **55**, 266-271.
127. W. Xu, X. Xue, T. Li, H. Zeng, X. Liu, *Angew. Chem. Int. Ed. Engl.*, 2009, **48**, 6849-6852.
128. C. D. Mol, C. F. Kuo, M. M. Thayer, R. P. Cunningham, J. A. Tainer, *Nature*, 1995, **374**, 381-386.
129. K. Okano and H. Kambara, *Anal. Biochem.*, **228**, 101-108.
130. H. Chen, J. Wang, G. Liang, P. Zhang, J. Kong, *Chem. Commun.*, 2012, **48**, 269-271.
131. X.-H. Zhao, Q.-J. Ma, X.-X. Wu, X. Zhu, *Anal. Chim. Acta*, 2012, **727**, 67-70.
132. X. Liu, R. Aizen, R. Freeman, O. Yehezkeli, I. Willner, *ACS Nano*, 2012, **6**, 3553-3563.
133. L. Peng, Z. Zhu, Han D., W. Tan, *Biosens. Bioelectron.*, 2012, **35**, 475-478.
134. C. Chen and B. Li., *Biosens. Bioelectron.*, 2014, **54**, 48-54.
135. Q. Wang, W. Wang, J. Lei, N. Xu, F. Gao, H. Ju, *Anal. Chem.*, 2013, **85**, 12182-12188.
136. L. Zhang, S. Guo, S. Dong, E. Wang, *Anal. Chem.*, 2012, **84**, 3568-3573.
137. J. Lu, I.T. Paulsen, D. Jin, *Anal. Chem.*, 2013, **85**, 8240-8245.
138. L. Cui, G. Ke, C. Wang, C. J. Yang, *Analyst*, 2010, **135**, 2069-2073.
139. R. Freeman, X. Liu, I. Willner, *NANO Lett.*, 2011, **11**, 4456-4461.
140. M. Zhang, Y.-M. Guan, B.-C. Ye, *Chem. Commun.*, 2011, **47**, 3478-3480.
141. C. J. Yang, L. Cui, J. Huang, L. Yan, X. Lin, C. Wang, *Biosens. Bioelectron.*, 2011, **27**, 119-124.
142. X. Zuo, F. Xia, Y. Xiao, K. W. Plaxco, *J. Am. Chem. Soc.*, 2010, **132**, 1816-1818.
143. X. Zuo, F. Xia, A. Patterson, H. T. Soh, Y. Xiao, K. W. Plaxco, *Chembiochem*, 2011, **12**, 2745-2747.
144. A. Zheng, M. Luo, D. Xiang, X. Xiang, X. Ji, Z. He, *Talanta*, 2013, **114**, 49-53.
145. C. Zhao, L. Wu, J. Ren, X. Qu, *Chem. Commun.*, 2011, **47**, 5461-5463.
146. J. Chen, J. Lin, S. Cai, D. Wu, C. Li, S. Yang, J. Zhang, *Anal. Chim. Acta*, 2014, **817**, 42-47.
147. X. Liu, Q. Xue, Y. Ding, J. Zhu, L. Wang, W. Jiang, *Analyst*, 2014, doi: 10.1039/c4an00389f.
148. Y. Gao and B. Li, *Anal. Chem.*, 2013, **85**, 11494-11500.
149. L. Cui, G. Ke, W. Y. Zhang, C. J. Yang, *Biosens. Bioelectron.*, 2011, **26**, 2796-2800.
150. S. Bi, L. Li, Y. Cui, *Chem. Commun.*, 2012, **48**, 1018-1020.
151. W. Zhou, X. Gong, Y. Xiang, R. Yuan, Y. Chai, *Biosens. Bioelectron.*, 2014, **55**, 220-224.
152. D. Wu, B.-C. Yi, B.-C. Ye, *Biosens. Bioelectron.*, 2011, **28**, 232-238.
153. C. Luo, H. Tang, W. Cheng, L. Yan, D. Zhang, H. Ju, *Biosens. Bioelectron.*, 2013, **48**, 132-137.
154. R. Miranda-Castro, D. Marchal, B. Limoges, F. Mavre, *Chem. Commun.*, 2012, **48**, 8772-8774.
155. J. Su, H. Zhang, B. Jiang, H. Zheng, Y. Chai, R. Yuan, Y. Xiang, *Biosens. Bioelectron.*, 2011, **29**, 184-188.
156. Y. Chen, B. Jiang, Y. Xiang, Y. Chai, R. Yuan, *Chem. Commun.*, 2011, **47**, 12798-12800.

157. Q. Fan, J. Zhao, H. Li, L. Zhu, G. Li, *Biosens. Bioelectron.*, 2012, **33**, 211-215.
158. R.-M. Kong, Z.-L. Song, H.-M. Meng, X.-B. Zhang, G.-L. Shen, R.-Q. Yu, *Biosens. Bioelectron.*, 2014, **54**, 442-447.
159. F. Xuan, X. Luo, I.-M. Hsing, *Anal. Chem.*, 2012, **84**, 5216-5220.
160. S. Liu, Y. Lin, L. Wang, T. Liu, C. Cheng, W. Wei, B. Tang, *Anal. Chem.*, 2014, **86**, 4008-4015.
161. S. Liu, C. Wang, C. Zhang, Y. Wang, B. Tang, *Anal. Chem.*, 2013, **85**, 2282-2288.
162. C. Lin, Y. Wu, F. Luo, D. Chen, X. Chen, *Biosens. Bioelectron.*, 2014, **59**, 365-369.
163. H. J. Lee, Y. Li, A. W. Wark, R. M. Corn, *Anal. Chem.*, 2005, **77**, 5096-5100.
164. S. M. Yoo, T. Kang, H. Kang, H. Lee, M. Kang, S. Y. Lee, B. Kim, *Small*, 2011, **7**, 3371-3376.
165. J. W. Little, *Gene Amplif. Anal.*, 1981, **2**, 135-145.
166. K. S. Sriprakash, N. Lundh, M. Moonhuh, C. M. Radding, *J. Biol. Chem.*, 1975, **250**, 5438-5445.
167. K. Hsieh, Y. Xiao, T. Soh, *Langmuir*, 2010, **26**, 10392-10396.
168. H. Xu, L. Wang, H. Ye, L. Yu, X. Zhu, Z. Lin, G. Wu, X. Li, X. Liu, G. Chen, *Chem. Commun.*, 2012, **48**, 6390-6392.
169. L. Liu, J. Lei, F. Gao, H. Ju, *Talanta*, 2013, **115**, 819-822.
170. J. A. Dougan, D. MacRae, D. Graham, K. Faulds, *Chem. Commun.*, 2011, **47**, 4649-4651.
171. R. J. Crouch, J. J. Toulme (eds) (1998). Ribonucleases H, Paris: John Libbey.
172. P. Duck, G. Alvarado-Urbina, B. Burdick, B. Collier, *Biotechniques*, 1990, **9**, 142-148.
173. H. H. Hogrefe, R. I. Hogrefe, J. A. Wlder, *J. Biol. Chem.*, 1990, **265**, 5561-5566.
174. M. L. Beggs, M. D. Cave, L. Cloney, C. Marlowe, P. Duck, K. D. Eisenach, *J. Clin. Microbiol.*, 1996, **34**, 2985-2989.
175. F. Bekkaoui, J. P. McNevin, C. H. Leung, G. J. Peterson, A. Patel, R. S. Bhatt, R. N. Bryan, *Diagn. Microbiol. Infect. Dis.*, 1999, **34**, 83-90.
176. W. K. Fong, Z. Modrusan, J. P. Mcnevin, J. Marostenmaki, B. Zin, F. Bekkaoui, *J. Clin. Microbiol.*, 2000, **38**, 2525-2529.
177. J. Merlino, B. Rose, C. Harbour, *Eur. J. Clin. Microbiol. Infect. Dis.*, 2003, **22**, 322-323.
178. Z. Modrusan, C. Marlowe, D. Wheeler, M. Pirseyedi, R. N. Bryan, *Diagn. Microbiol. Infect. Dis.*, 2000, **37**, 45-50.
179. S. Warnon, N. Zammattéo, I. Alexandre, C. Hans, J. Remacle, *Biotechniques*, 2000, **28**, 1152-1160.
180. L. T. Dickinson, D. C. Mah, R. T. Poirier, F. Bekkaoui, W. E. Lee, D. E. Bader, *Mol. Cell Probes.*, 2004, **18**, 341-348.
181. T. Tang, M. Y. Badal, G. Ocvirk, W. E. Lee, D. E. Bader, F. Bekkaoui, D. J. Harrison, *Anal. Chem.*, 2002, **74**, 725-733.
182. J. J. Harvey, S. P. Lee, E. K. Chan, J. H. Kim, E.-S. Hwang, A.-Y. Cha, J. R. Knutson, M. K. Han, *Anal. Biochem.*, 2004, **333**, 246-255.
183. R. R. Garafutdinov, Iu. M. Nikonorov, D. A. Chemeris, B. N. Postrigan', O. V. Chubukova, R. F. Talipov, V. A. Vakhitov, A. V. Chemeris, *Bioorg. Khim.*, 2009, **35**, 665-673.
184. T. Jacroux, D. C. Rieck, R. Cui, Y. Ouyang, W.-J. Dong, *Anal. Biochem.*, 2013, **432**, 106-114.
185. J. Hou, X. Liu, J. Wang, J. Liu, T. Duan, *Anal. Biochem.*, 2007, **371**, 162-166.
186. X.-P. Liu, J.-L. Hou, J.-H. Liu, *Anal. Biochem.*, 2010, **398**, 83-92.
187. T. T. Goodrich, H. J. Lee, R. M. Corn, *Anal. Chem.*, 2004, **76**, 6173-6178.
188. T. T. Goodrich, H. J. Lee, R. M. Corn, *J. Am. Chem. Soc.*, 2004, **126**, 4086-4087.

189. J. H. Kim, R. A. Estabrook, G. Braun, B. R. Lee, N. O. Reich, *Chem. Commun.*, 2007, **45**, 4342-4344.
190. X. Xiao, C. Song, C. Zhang, X. Su, M. Zhao, *Chem. Commun.*, 2012, **48**, 1964-1966.
191. K. Nakagawa, T. Yamamoto, A. Yasuda, *Anal. Biochem.*, 2010, **404**, 165-170.
192. G. M. Myles and A. Sancar, *Chem. Res. Toxicol.*, 1989, **2**, 197-226.
193. D. A. Shagin, D. V. Rebrikov, V. B. Kozhemyako, I. M. Altshuler, A. S. Shcheglov, P. A. Zhulidov, E. A. Bogdanova, D. B. Staroverov, V. A. Rasskazov, S. Lukyanov, *Genome Res.*, 2002, **12**, 1935-1942.
194. B.-C. Yin, Y.-Q. Liu, B.-C. Ye, *J. Am. Chem. Soc.*, 2012, **134**, 5064-5067.
195. X. Lin, C. Zhang, Y. Huang, Z. Zhu, X. Chen, C. J. Yang, *Chem. Commun.*, 2013, **49**, 7243-7245.
196. T. Tian, H. Xiao, Z. Zhang, Y. Long, S. Peng, S. Wang, X. Zhou, S. Liu, X. Zhou, *Chem. Eur. J.*, 2013, **19**, 92-95.
197. S. Vanecko and M. Laskowski, *J. Biol. Chem.*, 1961, **236**, 3312-3316.
198. Z. Tang, H. Wu, J. R. Cort, G. W. Buchko, Y. Zhang, Y. Shao, I. A. Aksay, J. Liu, Y. Lin, *Small*, 2010, **6**, 1205-1209.
199. L. Cui, X. Lin, N. Lin, Y. Song, Z. Zhu, X. Chen, C. J. Yang, *Chem. Commun.*, 2012, **48**, 194-196.
200. H. Wang, S. Wu, X. Chu, R.-Q. Yu *Chem. Commun.*, 2012, **48**, 5916-5918.